

## 111. Formation of Heptaleno[1,2-*c*]furans and Heptaleno[1,2-*c*]furanones

by Peter Uebelhart, Peter Mohler, Reza-Ali Fallahpour<sup>1)</sup> and Hans-Jürgen Hansen\*

Organisch-chemisches Institut der Universität, Winterthurerstrasse 190, CH-8057 Zürich

(21. VII. 95)

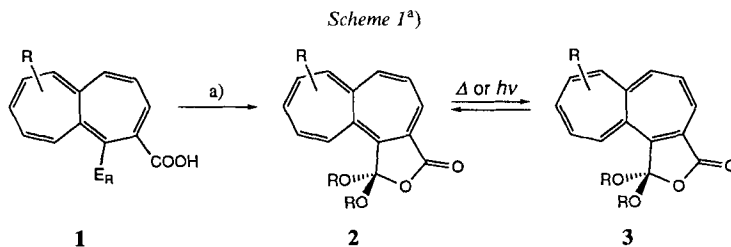
The dehydrogenation reaction of the heptalene-4,5-dimethanols **4a** and **4d**, which do not undergo the double-bond-shift (DBS) process at ambient temperature, with basic MnO<sub>2</sub> in CH<sub>2</sub>Cl<sub>2</sub> at room temperature, leads to the formation of the corresponding heptaleno[1,2-*c*]furans **6a** and **6d**, respectively, as well as to the corresponding heptaleno[1,2-*c*]furan-3-ones **7a** and **7d**, respectively (cf. Scheme 2 and 8). The formation of both product types necessarily involves a DBS process (cf. Scheme 7). The dehydrogenation reaction of the DBS isomer of **4a**, i.e., **5a**, with MnO<sub>2</sub> in CH<sub>2</sub>Cl<sub>2</sub> at room temperature results, in addition to **6a** and **7a**, in the formation of the heptaleno[1,2-*c*]furan-1-one **8a** and, in small amounts, of the heptalene-4,5-dicarbaldehyde **9a** (cf. Scheme 3). The benzo[*a*]heptalene-6,7-dimethanol **4c** with a fixed position of the C=C bonds of the heptalene skeleton, on dehydrogenation with MnO<sub>2</sub> in CH<sub>2</sub>Cl<sub>2</sub>, gives only the corresponding furanone **11b** (Scheme 4). By [<sup>2</sup>H<sub>2</sub>]-labelling of the methanol function at C(7), it could be shown that the furanone formation takes place at the stage of the corresponding lactol [3-<sup>2</sup>H<sub>2</sub>]-**15b** (cf. Scheme 6). Heptalene-1,2-dimethanols **4c** and **4e**, which are, at room temperature, in thermal equilibrium with their corresponding DBS forms **5c** and **5e**, respectively, are dehydrogenated by MnO<sub>2</sub> in CH<sub>2</sub>Cl<sub>2</sub> to give the corresponding heptaleno[1,2-*c*]furans **6c** and **6e** as well as the heptaleno[1,2-*c*]furan-3-ones **7c** and **7e** and, again, in small amounts, the heptaleno[1,2-*c*]furan-1-ones **8c** and **8e**, respectively (cf. Scheme 8). Therefore, it seems that the heptalene-1,2-dimethanols are responsible for the formation of the furan-1-ones (cf. Scheme 7). The methylenation of the furan-3-ones **7a** and **7e** with *Tebbe's* reagent leads to the formation of the 3-methyl-substituted heptaleno[1,2-*c*]furans **23a** and **23e**, respectively (cf. Scheme 9). The heptaleno[1,2-*c*]furans **6a**, **6d**, and **23a** can be resolved into their antipodes on a *Chiralcel OD* column. The (*P*)-configuration is assigned to the heptaleno[1,2-*c*]furans showing a negative *Cotton* effect at ca. 320 nm in the CD spectrum in hexane (cf. Figs. 3–5 as well as Table 7). The (*P*)-configuration of (–)-**6a** is correlated with the established (*P*)-configuration of the dimethanol (–)-**5a** via dehydrogenation with MnO<sub>2</sub>. The degree of twisting of the heptalene skeleton of **6** and **23** is determined by the Me-substitution pattern (cf. Table 9). The larger the heptalene *gauche* torsion angles are, the more hypsochromically shifted is the heptalene absorption band above 300 nm (cf. Table 7 and 8, as well as Figs. 6–9).

**1. Introduction.** – Several years ago, we described the synthesis of cyclic 'ortho'-anhydrides (pseudo-esters) **2** of heptalene-4,5-dicarboxylic acids<sup>2)</sup> by reaction of the corresponding mono-esters with the *in situ* generated iminium salt of DMF and oxalyl chloride, followed by addition of ROH [3–5] (Scheme 1)<sup>3)</sup>. Similarly, the isomeric 4-(alkoxy-carbonyl)heptalene-5-carboxylic acids give the corresponding isomeric 'ortho'-anhydrides and their double-bond-shifted (DBS) forms (cf. [4]). These 'ortho'-anhydrides represent 1,1-dialkoxyheptaleno-furan-3-ones, **2** and **3**, and 3,3-dialkoxyheptaleno-furan-1-ones, respectively. Since they can be regarded in their reduced forms as furano analogues of colchicinoids, we were interested in the synthesis of such compounds. For this

<sup>1)</sup> New address: Institut für Anorganische Chemie der Universität, Spitalstrasse 51, CH-4056 Basel.

<sup>2)</sup> The new numbering of heptalene is applied (cf. R-2.4.3.3 in [1] as well as Footnote 2 in [2]).

<sup>3)</sup> The method was originally developed by *Stadler* [6] for the mild and efficient esterification of protected  $\alpha$ -amino acids which does not lead to partial racemization.

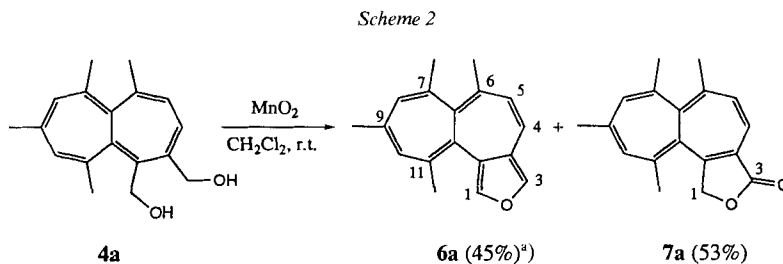


a) 1. DMF +  $\text{COCl}_2/\text{MeCN}$ ,  $0^\circ$ ; 2. ROH/MeCN,  $0^\circ$ .

<sup>a)</sup>  $\text{E}_R = \text{COOR}$  in this and the following Schemes.

purpose, we studied the dehydrogenation reaction of heptalene-4,5- and heptalene-1,2-dimethanols, which can easily be obtained by  $\text{LiAlH}_4$  or DIBAH reduction of the corresponding heptalene-dicarboxylates, with activated  $\text{MnO}_2$  in  $\text{CH}_2\text{Cl}_2$  (*cf.* [7]).  $\text{MnO}_2$  has already successfully been applied for the synthesis of lactones from corresponding dimethanols (*cf.* [7] and in particular [8]). Moreover, we have found that 2-(hydroxymethyl)-1-methylazulenes can be reacted with  $\text{MnO}_2$  in  $\text{CH}_2\text{Cl}_2$  to give azulene-2-carbaldehydes as well as azulene-1,2-dicarbaldehydes (*cf.* [9] and lit. cit. therein).

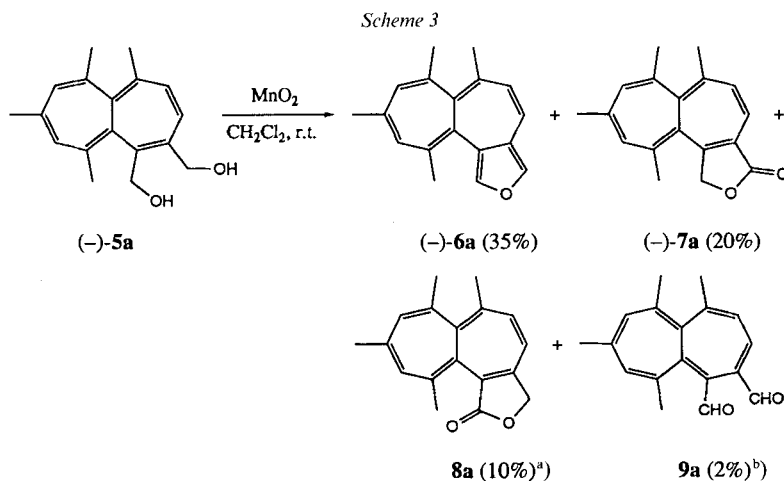
**2. Formation of Heptaleno[1,2-*c*]furans and -furanones.** The heptalene-4,5-dimethanol which is stable with respect to the thermal DBS process, at least at temperatures  $< 80^\circ$  [3] [10], served together with its DBS isomer **5a** as model compound. When **4a** was vigorously stirred in  $\text{CH}_2\text{Cl}_2$  at room temperature in the presence of a 20–25-fold amount by weight of  $\text{MnO}_2$ <sup>4)</sup>, it was completely consumed within 30–40 min. Two products could be isolated, after removal and extraction of  $\text{MnO}_2$  with  $\text{CH}_2\text{Cl}_2$ , by chromatography on silica gel, namely the heptaleno[1,2-*c*]furan **6a** and the heptaleno[1,2-*c*]furan-3-one **7a** (Scheme 2). A closer inspection of the course of the reaction by TLC revealed the presence of intermediate products, too labile to be isolated by preparative TLC. On standing of the  $\text{CH}_2\text{Cl}_2$  solution at room temperature, these intermediate products vanished in favor of



<sup>a)</sup> The yields, given in parentheses in this and the other Schemes, refer to pure chromatographed material. They were obtained with basic  $\text{MnO}_2$  [11] after 40 min vigorous stirring and treatment of the filtered  $\text{CH}_2\text{Cl}_2$  solution with a catalytic amount of TsOH for 3 h at room temperature (*cf. Exper. Part*).

<sup>4)</sup> We performed our first experiments with an old batch of 'Mangan(IV)-oxid, gefällt, aktiv' from Merck-Schuchardt (*cf.* [9]). Later, we found that basic  $\text{MnO}_2$ , prepared according to [11], led to better reproducible results.

the formation of **6a** and possibly **7a**. The addition of a trace of TsOH to the  $\text{CH}_2\text{Cl}_2$  solution promoted the disappearance of the intermediate products by concomitant enlargement of the spot of **6a** on TLC. We concluded from these observations that a hemi-aldehyde of **4a** or a corresponding DBS form of this hemialdehyde as well as their corresponding ring-closed lactol forms are present which, on 1,4-elimination of  $\text{H}_2\text{O}$ , give **6a** and, on further dehydrogenation, lead to the formation of **7a** or its DBS form, which, on thermal double-bond shift, affords **7a** (see later). Since the structure of both isolated compounds **6a** and **7a** reveals that they are, with respect to the starting compound **4a**, DBS forms, we investigated the behavior of the corresponding isomeric 1,2-dimethanol **5a**, with the  $\text{C}=\text{C}$  bonds already in the 'right' position, in the presence of  $\text{MnO}_2$  in  $\text{CH}_2\text{Cl}_2$  (Scheme 3). Indeed, we performed the dehydrogenation reaction with the (–)-(*P*)-enantiomer of **5a**, which was available from former work [3] [12]. The result was similar to that with the DBS form of **5a**; however, the yields of the furan **6a** and the furanone **7a** were definitely lower, and we observed the formation of two other isolable products, namely the heptaleno-furan-1-one **8a** and the heptalene-4,5-dicarbaldehyde **9a**. After chromatography, the latter two compounds were only obtained in a *ca.* 4:1 mixture. However, their structures could be deduced from their  $^1\text{H-NMR}$  data (see *Chapt. 3*). The observation that a dicarbaldehyde **9a** is formed in the  $\text{MnO}_2$  reaction of **5a** opens, in principle, a new way for the formation of the furanones **7a** and **8b**, since they are on the same oxidation level as **9a**. An intramolecular type of *Cannizzaro* reaction similar to the *Tischchenko* reaction of **9a** could result in the formation of **7a** and **8a**. However, at the moment, we have no indication that **9a** can easily be transformed into **7a** and/or **8a**<sup>5</sup>). Since DBS processes, which presumably occur on the level of five-ring intermediates of the lactol or

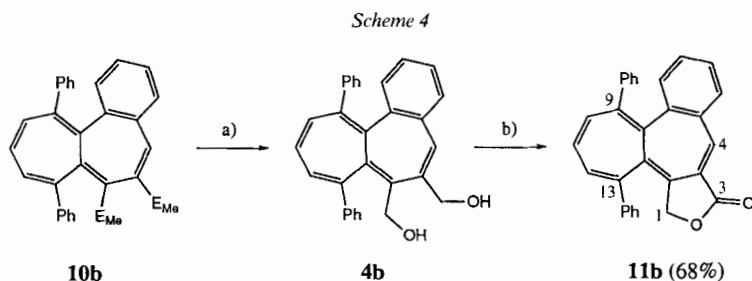


<sup>a)</sup> Obtained in a *ca.* 4:1 mixture with **9a**. The optical activity was not determined. It should be similar to that of (–)-**7a** with two negative CE (*Cotton* effect) above 300 nm (see later).

<sup>b)</sup> The structure of **9a** could unequivocally be established by its  $^1\text{H-NMR}$  spectrum in the 1:4 mixture with **8a** (see *Exper. Part*).

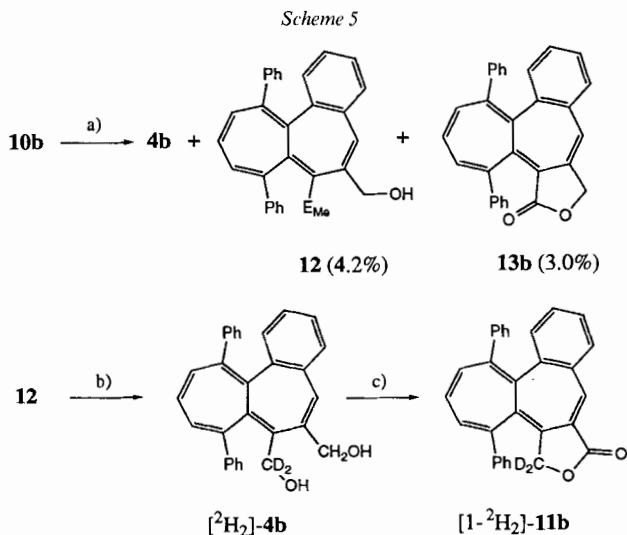
<sup>5)</sup> Treatment of the 4:1 mixture **8a/9a** in  $\text{CDCl}_3$  with  $\text{Et}_3\text{N}$  did not change its composition. Addition of traces of  $\text{CF}_3\text{COOH}$  destroyed **9a**.

lactone type (*cf.* [4] [5]), are accompanying the dehydrogenation reactions of **4a** and **5a** at room temperature, we studied the dehydrogenation reaction of the benzo[*a*]heptalene-6,7-dimethanol **4b**, which is available by DIBAH reduction of the corresponding benzo[*a*]heptalene-6,7-dicarboxylate **10b** (*cf.* also *Scheme 5*) [13], and which possesses a fixed position of the C=C bonds in the heptalene perimeter due to the benzo annelation (*Scheme 4*). The outcome of this reaction was unambiguous. Only furanone **11b** was formed in an isolated yield of 68%, and no trace of its isomer **13b** (*cf.* *Scheme 5*) was detectable by <sup>1</sup>H-NMR spectroscopy in the crude mixture. On the other hand, two sharp *s* at 9.78 and 9.70 ppm (CDCl<sub>3</sub>) as well as a *s* at 8.14 and a *d* (*J* = 7.7 Hz) at 7.60 ppm (the ratio of the integrals of the 4 signals amounted to 1:1.1:1) indicated the presence of a further product, which disappeared within 12 h on standing of the CDCl<sub>3</sub> solution at



a) 20% DIBAH in hexane/THF, 0°; 89% (see also *Scheme 5*).

b) 20-fold amount by weight of MnO<sub>2</sub> with respect to **4b**; CH<sub>2</sub>Cl<sub>2</sub>, room temperature, 2 h.



a) See *a)* in *Scheme 4*.

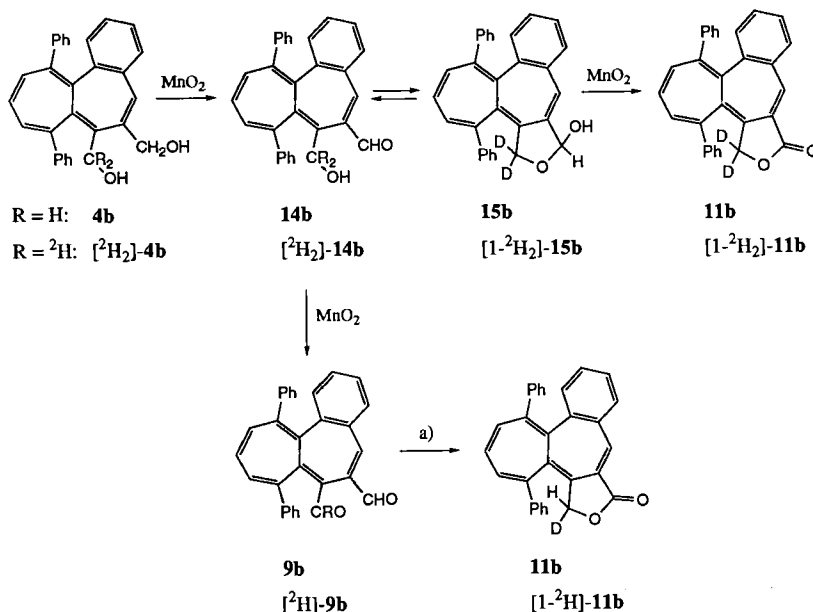
b) LiAl[<sup>2</sup>H<sub>4</sub>]/THF, room temperature; quant.

c) 19-fold amount by weight of MnO<sub>2</sub>/CH<sub>2</sub>Cl<sub>2</sub>, room temperature, 2 h; 58%.

room temperature. At the end, only the  $^1\text{H-NMR}$  signals of the furanone **11b** with its characteristic *AB* system of  $\text{CH}_2(1)$  at 4.47 and 3.93 ppm and  $^2J_{AB} = 13.2$  Hz (see also *Chapt. 3*) were recognizable.

The *s* signals at 9.78, 9.70, and 8.14 ppm, and the *d* at 7.60 ppm are due, we assume, to the H-atoms of two aldehyde groups and to H–C(5) and H–C(4) of the corresponding 6,7-dicarbaldehyde **9b** of **4b**. To prove whether this dicarbaldehyde is a necessary intermediate for the formation of **11b** or not, we synthesized  $[\text{}^2\text{H}_2]\text{-4b}$  from a side-product **12** of the reduction of **10** with DIBAH (*Scheme 5*). Its dehydrogenation with  $\text{MnO}_2$  in  $\text{CH}_2\text{Cl}_2$  gave exclusively  $[\text{}^1\text{-}^2\text{H}_2]\text{-11b}$ . This experiment shows that **9b** is not a necessary intermediate for the formation of **11b**, and that the main source of **11b** must be the corresponding lactol **15b**, which is further dehydrogenated by  $\text{MnO}_2$  to lead to lactone **11b** (*Scheme 6*), as it had been postulated in other cases (see [7] and, in particular, [8]). Therefore, we

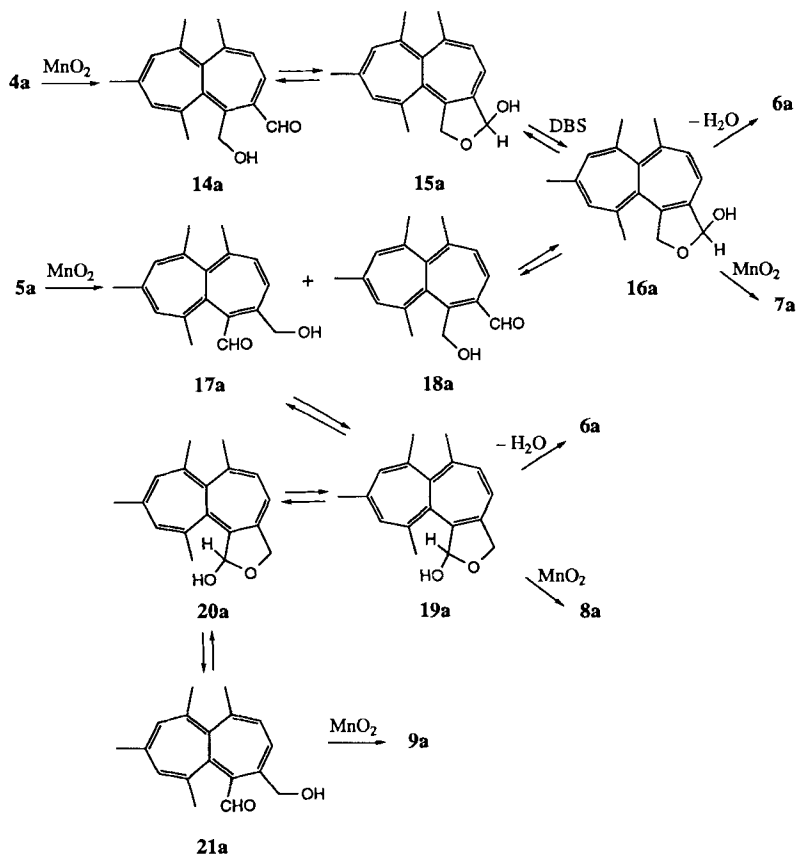
Scheme 6



a) Acid- or base-catalyzed intramolecular *Camizzaro* reaction.

assume that the formation of **7a** in the case of the dehydrogenation of **4a** (*Scheme 2*) as well as the formation of **7a** and **8a** from **5a** (*Scheme 3*) involves the corresponding lactols (*Scheme 7*). The fact that **4a** gives only the furanone **7a**, its DBS isomer **5a**, however, **7a** as well as **8a**, can be interpreted as a result of a different chemoselectivity of the  $\text{MnO}_2$  reaction with **4a** and **5b**. *Scheme 7* combines the most probable pathways for the formation of the furan **6a**, the furanones **7a** and **8a**, as well as the dicarbaldehyde **9a**, taking into account that DBS processes will most likely take place only in the cyclized lactol forms **15a** and **16a** as well as **19a** and **20a**. However, we have also to bear in mind that the experiment with  $[\text{}^2\text{H}_2]\text{-4b}$  does not completely rule out the possibility that also the

Scheme 7

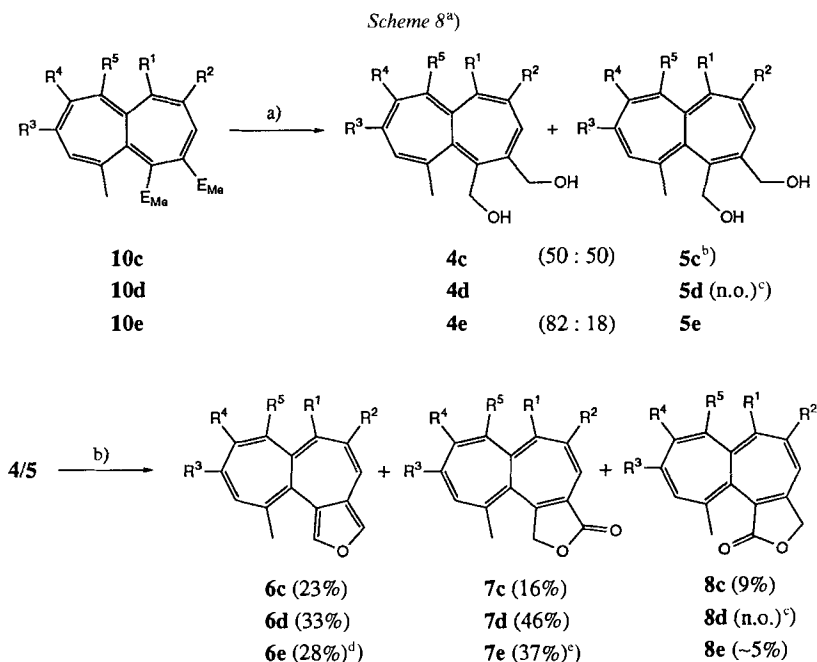


dicarbaldehyde **9a** or its DBS isomer leads to furanone **7a** and possibly **8a** (*cf. Scheme 6*). If we assume an appreciable primary  $^1\text{H}/^2\text{H}$  isotope effect in the dehydrogenation reactions **14b**  $\rightarrow$  **9b**/ $[\text{}^2\text{H}_2]$ -**14b**  $\rightarrow$   $[\text{}^2\text{H}]$ -**9b**, the latter reaction may have no change to compete with the cyclization reaction to  $[\text{}^2\text{H}_2]$ -**15b**, followed by the dehydrogenation to the labelled furanone  $[\text{}^2\text{H}_2]$ -**11b**<sup>6</sup>). We will come back to this point in a later communication.

The outcome of the dehydrogenation reaction of other heptalene-4,5- and heptalene-1,2-dimethanols by  $\text{MnO}_2$  in  $\text{CH}_2\text{Cl}_2$  is delineated in *Scheme 8*. As can be seen, the side-by-side formation of the corresponding heptaleno[1,2-*c*]furans and -furan-3-ones is observed in all three cases. However, in two cases, we had to experiment with the thermal equilibrium mixture of the heptalene-4,5- and heptalene-1,2-dimethanols which was readily established already at room temperature. In these two instances, the formation of the corresponding furan-1-ones (see **8c** and **8e**) took also place. The mixture **4c/5c** was

<sup>6</sup>) Indeed, in the dehydrogenation reaction of 2-(hydroxymethyl)-4,6,8-trimethylazulene and its 2-(hydroxy- $[\text{}^2\text{H}_2]$ methyl) isotopomer with  $\text{MnO}_2$  in  $\text{CH}_2\text{Cl}_2$ , we observed a corresponding  $^1\text{H}/^2\text{H}$  isotope effect (*cf. [14]*).

quite unstable, and we had to dehydrogenate the crude reaction mixture just after reduction of the heptalene-dicarboxylate **10c**, which, in turn, represented already a thermal equilibrium mixture at room temperature with 27.5% of the DBS form of **10c** in equilibrium [15]<sup>7</sup>). The <sup>1</sup>H-NMR analysis of the crude 1:1 mixture **4c/5c** showed that this mixture contained already a small amount of the furan-1-one **8c**. A similar control experiment with the crude mixture **4e/5e** indicated that the DIBAH reduction of the heptalene-4,5-dicarboxylate **10e** occurred without formation of the furan-1-one **8e**. Treatment of the 82:18 mixture **4e/5e** with MnO<sub>2</sub> led to formation of a product mixture, which contained, according to <sup>1</sup>H-NMR analysis, 50% of the heptaleno[1,2-*c*]furan **6e**, 46% of the thermal equilibrium mixture of **7e** and its DBS isomer (see *Scheme 8*), and 4% of **8e**. All these results are in line with the outcome of the model experiments with **4a** and **5a** (see *Scheme 3* and *4*). They demonstrate that MnO<sub>2</sub> in CH<sub>2</sub>Cl<sub>2</sub> dehydrogenate, at room



a) See a) in *Scheme 4* and *Exper. Part*.

b) 30-fold amount by weight of MnO<sub>2</sub>/CH<sub>2</sub>Cl<sub>2</sub>, room temperature.

a) c: R<sup>1</sup>, R<sup>4</sup> = H, R<sup>2</sup>, R<sup>3</sup>, R<sup>5</sup> = Me; d: R<sup>4</sup> = H, R<sup>1</sup>, R<sup>2</sup>, R<sup>3</sup>, R<sup>5</sup> = Me; e: R<sup>2</sup>, R<sup>3</sup>, R<sup>5</sup> = H, R<sup>1</sup> = Me, R<sup>4</sup> = *i*-Pr.

b) The crude mixture **4e/5e** contained already a small amount of **8c** (2–3%). This mixture was directly reacted with MnO<sub>2</sub>.

c) n.o. = not observed.

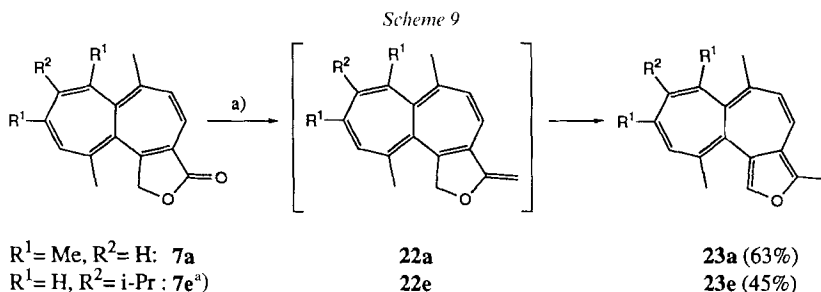
d) According to <sup>1</sup>H-NMR of a crude reaction mixture, the ratio **6e/7e/8e** amounted to 50:46:4.

e) In thermal equilibrium at room temperature, with 22% of its DBS isomer **11e**.

<sup>7)</sup> Similarly, *Knaup* [16] observed in the reaction of 6,8,10-trimethylheptalene-4,5-dimethanol, which should already contain its 1,2-dimethanol form, with BaMnO<sub>4</sub> in boiling CH<sub>2</sub>Cl<sub>2</sub> the formation of all three product types.

temperature, the heptalene-4,5-dimethanols **4** chemoselectively at the sterically less hindered methanol function at C(4) (C(6) in **4b**), thus leading to the corresponding 4-carbaldehydes **14** (cf. *Scheme 6* and *7*), which, on cyclization to the corresponding lactols **15**, give rise to the reversible formation of their DBS forms **16**. The latter compounds can undergo a further dehydrogenation reaction by  $\text{MnO}_2$  to give the furanones **7** and, in competition by 1,4-elimination of  $\text{H}_2\text{O}$ , the corresponding furans **6**. The smooth reaction of the 6,7-dimethanol **4b** with  $\text{MnO}_2$  shows that, as expected, the second dehydrogenation reaction can also take place on the level of the lactols **15**. Therefore, it might be that furanones of type **11** (cf. *Scheme 6*) are formed in all cases, and that the concluding DBS process finally leads to the furanones **7**<sup>8</sup>). In contrast to the dehydrogenation reaction of the heptalene-4,5-dimethanols **4**, their DBS forms **5** seem to react with  $\text{MnO}_2$  at both methanol functions, thus leading to a mixture of the carbaldehydes **17** and **18** (cf. *Scheme 7*). The amount of **17** in the mixture **17/18** may be higher than reflected by the isolated amount of the furanones **8**, since the expected lactols **19** arising from **17** by cyclization may undergo a competitive dehydrogenation reaction by  $\text{MnO}_2$  to give the furanones **8** and a 1,4-elimination of  $\text{H}_2\text{O}$ , resulting in the formation of the furans **6**, which will also be formed *via* **18** and their DBS forms **16** (cf. *Scheme 7*).

The furan-3-ones **7** allow the synthesis of other furans<sup>9</sup>). Two examples are shown in *Scheme 9*. It is known that lactones can be methylated with *Tebbe's* reagent at their oxo



a) 1 mol-equiv. of *Tebbe* reagent (Aldrich<sup>®</sup>) in 0.5M solution in toluene, room temperature; followed by basic workup (cf. *Exper. Part*).

<sup>a</sup>) Thermal equilibrium mixture of 78% of **7e** and 22% of **11e**.

<sup>8</sup>) The high chemoselectivity of the dehydrogenation reaction of the heptalene-4,5-dimethanols is in keeping with corresponding nucleophilic addition reaction to heptalene-4,5-dicarboxylates, which takes place nearly exclusively at the  $\text{MeOCO}$  group at C(4). Examples are the selective saponification of heptalene-4,5-dicarboxylates with  $\text{KOH}$  in  $\text{EtOH}/\text{H}_2\text{O}$  mixtures [3] as well as their reaction with *Tebbe's* reagent [17] and the carbanion of methanesulfone-morpholide [17]. On the other hand, due to the complexity of the possible reaction paths of **4** and **5** (cf. *Scheme 7*), we cannot completely rule out the eventuality that the dehydrogenation reaction of **4** leads also to some extent to the isomeric 5-carbaldehydes **21**. For such a case, we have to postulate that their cyclized lactol forms **20** undergo rapid elimination of  $\text{H}_2\text{O}$  with concomitant shift of the  $\text{C}=\text{C}$  bonds in the heptalene perimeter to give directly the furans **6**, since the formation of the furan-1-ones **8** was not observed with 4,5-dimethanols. However, at the moment we have no reason to assume that the '1,14-elimination' of  $\text{H}_2\text{O}$  in **20** proceeds with more ease than the 1,4-elimination of  $\text{H}_2\text{O}$  in **16** (cf. *Scheme 7*).

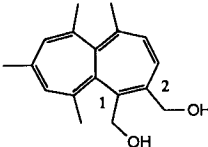
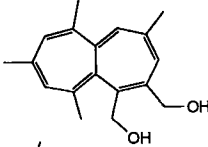
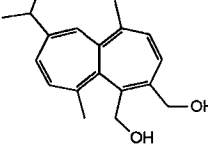
<sup>9</sup>) First results of the reduction of **7a** with  $\text{DIBALH}$  at temperatures below  $-60^\circ$  show that it can be reduced to the corresponding lactol **16a**, which, on workup, yields just heptaleno-furan **6a**. However, the yields are still < 30%.



function (*cf.* [18]). Similarly, when the furan-3-ones **7a** and **7e** were reacted with 1 mol-equiv. of *Tebbe's* reagent in toluene, we observed a smooth formation of the corresponding 3-methyl-substituted heptaleno[1,2-*c*]furans **23a** and **23e**, respectively. Intermediates are most probably the methylene forms **22a** and **22e**, which isomerize under base catalysis to the final products. No other products were observed.

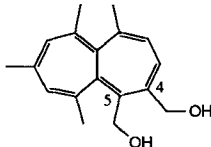
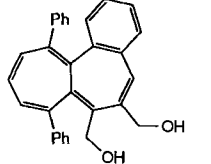
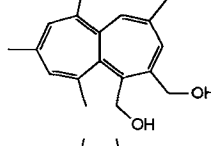
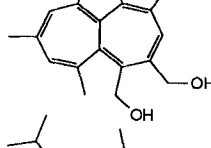
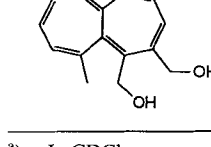
**3. Spectroscopic and Chiroptical Properties of the New Compounds.** – 3.1. *Heptalene-4,5- and Heptalene-1,2-dimethanols*. The structure of the heptalene-dimethanols is clearly assignable on the basis of the structure of the starting materials, *i.e.*, the corresponding heptalene-dicarboxylates (*cf.* [3]). However, in the case of the reduction of the heptalene-dicarboxylates **10c** and **10e**, a thermal equilibrium mixture of the heptalene-4,5- and heptalene-1,2-methanols **4c/5c** and **4e/5e**, respectively, is obtained (*cf. Scheme 8*). Of course, in the instance of the pair **4e/5e**, the vicinal coupling constants of H–C(2), H–C(3) and H–C(7), H–C(8) in **4e** and of H–C(3), H–C(4) and H–C(8), H–C(9) in **5e** in the order 6.1–6.3 and 11.5–12.5 Hz, respectively, define unequivocally the position of the C=C bonds of the heptalene skeleton. However, the pair **4c/5c** does not possess such adjacent H-atoms at the heptalene skeleton. Nevertheless, an assignment of the structure is possible unambiguously. Both series of heptalene-dimethanols exhibit in each case two sets of clearly distinguishable *AB* systems for the corresponding diastereotopic H-atoms of the CH<sub>2</sub>OH group at C(1) and C(2) in **5** and at C(5) and C(4) of **4** (*cf. Table 1* and 2). The heptalene-1,2-dimethanols are characterized by a much larger chemical-shift difference ( $\Delta\delta$ ) of the H-atoms of the CH<sub>2</sub>OH group at C(1) ( $\Delta\delta \geq 0.5$  ppm) as compared to that of the H-atoms of the CH<sub>2</sub>OH group at C(2) ( $\Delta\delta \leq 0.32$  ppm). We assume that the

Table 1. *Chemical Shifts [ppm] and Geminal Coupling Constants [Hz] of the AB Systems of the CH<sub>2</sub>OH Groups in Heptalene-1,2-dimethanols 5*

Dimethanol	$\delta(\text{CH}_2\text{-C(1)})^a$		$\delta(\text{CH}_2\text{-C(2)})$		$^2J(\text{CH}_2\text{-C(1)})$	$^2J(\text{CH}_2\text{-C(2)})$	
	A(1)	B(1)	A(2)	B(2)			
	<b>5a</b>	4.60	4.04	4.48	4.19	12.7	12.0
	<b>5c</b>	4.61	4.10	4.49	4.24	13.2	12.2
	<b>5e</b>	4.59	4.09	4.50	4.28	12.9	12.0

<sup>a</sup>) In CDCl<sub>3</sub>.

Table 2. Chemical Shifts [ppm] and Geminal Coupling Constants [Hz] of the AB Systems of the CH<sub>2</sub>OH Groups in Heptalene-4,5-dimethanols **4**

Dimethanol	$\delta(\text{CH}_2\text{-C}(5))^a$	$\delta(\text{CH}_2\text{-C}(4))$	$^2J(\text{CH}_2\text{-C}(5))$	$^2J(\text{CH}_2\text{-C}(4))$		
	<b>4a</b>	4.34	4.39	4.28	~ 12	12.6
	<b>4b</b>	4.19 <sup>b)</sup>	4.56	4.43	~ 13	12.4
	<b>4c</b>	4.28	4.35	4.31	n.d. <sup>c)</sup>	12.4
	<b>4d</b>	4.30	4.38	4.27	~ 12	12.6
	<b>4e</b>	4.33	4.37	4.29	~ 12	12.7

<sup>a)</sup> In CDCl<sub>3</sub>.

<sup>b)</sup> CH<sub>2</sub>-C(7) and CH<sub>2</sub>-C(6), respectively.

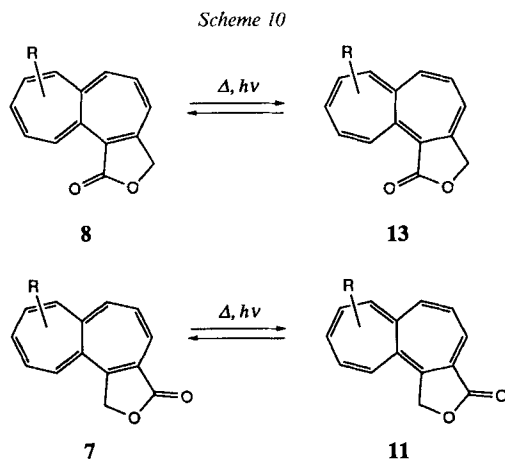
<sup>c)</sup> N.d. = not detectable.

shielding effect of the *s-trans*-oriented C(10)=C(10a) bond is responsible for this effect. The situation is just inverse for the heptalene-4,5-dimethanols **4**. Here show the H-atoms of the CH<sub>2</sub>OH group at the *peri*-position (C(5)) nearly the same chemical shifts and appear as a broad *s* with just recognizable satellite bands due to the <sup>2</sup>*J* coupling. Also the H-atoms of the CH<sub>2</sub>OH group at C(4) exhibit only a small chemical-shift difference of *ca.* 0.1 ppm.

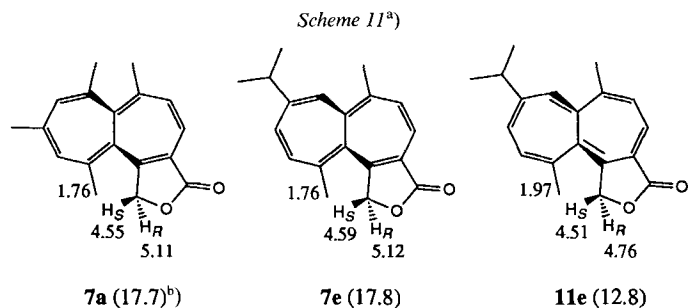
The assignment of the chemical shifts of the CH<sub>2</sub>OH groups is based on <sup>1</sup>H-NOE measurements as well as <sup>1</sup>H, <sup>13</sup>C correlation spectra and chemical correlations (see *Exper. Part*).

The (*P*)-configuration of (–)-**5** is correlated with the (*P*)-configuration of the corresponding heptalene-4,5-dicarboxylate (*cf.* [3] [10a]). The CD spectrum of (–)-**5a** is depicted in *Fig. 1* (*cf. Sect. 3.3*).

3.2. *Heptaleno[1,2-c]furan-3- and -1-ones*. The dehydrogenation reactions of the heptalene-4,5- and heptalene-1,2-dimethanols can, in principle, lead to the formation of four different types of furanones, namely, as we have seen, the furan-1-ones **8** and their DBS forms **13** as well as the furan-3-ones **7** and their DBS forms **11** (Scheme 10). It is



difficult to differentiate between these structures on the basis of their UV, IR, or mass spectra (see *Exper. Part*). Moreover, not all structural types with the same substitution pattern were available for a comparison of their spectral data. However, their  $^1\text{H-NMR}$  data always allowed an unambiguous assignment of their structure, also in those cases, where only  $^1\text{H-NMR}$  spectra of mixtures were available. The position of the  $\text{C}=\text{C}$  bonds at the heptalene skeleton could be derived directly from the observed vicinal  $\text{H,H}$ -coupling constants, where possible. The distinction of the furan-1-one and furan-3-one structures was possible on the basis of  $^1\text{H-NOE}$  experiments. Irradiation of the Me group at C(11) caused no  $^1\text{H-NOE}$  effect on the  $AB$  system of the  $\text{CH}_2$  H-atoms in the case of the furan-1-ones. On the other hand, the furan-3-ones **7** show a strong  $^1\text{H-NOE}$  effect only on the low-field H-atom of the  $AB$  system of the  $\text{CH}_2$  H-atoms (Scheme 11). Therefore, it



<sup>a)</sup> Stereochemical assignments are given for the (*P*)-configuration of the heptalene skeleton.

<sup>b)</sup>  $^2J(\text{H}_R, \text{H}_S)$  in Hz in parentheses.

is  $H_{RS}-C(1)$  at ca. 5.10 ppm ( $CDCl_3$ ) that lies in the  $\pi$  plane of the twisted *s-trans*-butadiene substructure ( $C(11)-C(11a)-C(11b)-C(3a)$ ) next to  $Me-C(11)$  in the furan-3-ones **7**.  $H_{SR}-C(1)$  is in a nearly orthogonal position with respect to the mentioned  $\pi$  plane and, therefore, absorbs at much higher field ( $\Delta\delta(H_{RS}-H_{SR}) = 0.55$  ppm; cf. Table 3). The DBS form **11e** of **7e** exhibits the *AB* system of  $CH_2(1)$  at 4.76 and 4.51 ppm, and it is again the H-atom at lower field that shows a  $^1H$ -NOE effect, when  $Me-C(11)$  at 1.97 ppm is irradiated. Therefore, it is once more  $H_{RS}-C(1)$  that appears at slightly lower field than  $H_{SR}-C(1)$  ( $\Delta\delta(H_{RS}-H_{SR}) = 0.2$  ppm; cf. Table 3).

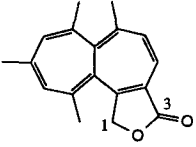
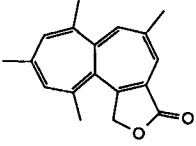
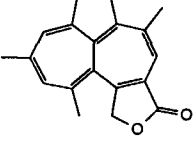
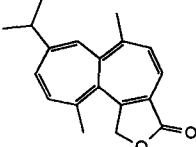
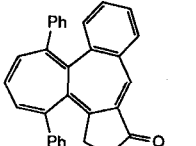
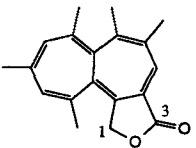
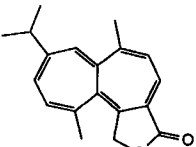
The differentiation between the two DBS forms **7** and **11** is quite generally possible on the basis of the observed geminal coupling constants of the  $CH_2$  H-atoms.  $^2J(H_{RS},H_{SR}) = 17.7$  Hz is, due to the homoconjugation of the  $CH_2$  H-C bonds with the lactone function *via* the  $C(3a)=C(11b)$  bond (cf. [19]), distinctly larger in the furanones **7** than in the corresponding DBS furanones **11** ( $^2J(H_{RS},H_{SR}) = 12.8$  Hz) with their reduced homoconjugation (cf. Table 3). A similar effect is observed for the furan-1-ones (cf. Table 4). Again, those furanones **8** with a strong homoconjugation between the H-C bonds of their  $CH_2$  group and the C=O group, due to the presence of a  $C(3a)=C(11b)$  bond, show a geminal coupling constant of the  $CH_2$  H-atoms in the order of 17 Hz. When there is no C=C bond between  $C(3a)$  and  $C(11b)$ , the geminal coupling constant of the  $CH_2$  H-atoms is anew reduced to 13 Hz as shown at least by the sole example (**13b**) we have had measured (cf. Table 4). As expected, the furan-3-ones **7** exhibit also much larger  $\Delta\delta$  values (0.55 ppm) of their  $CH_2$  H-atoms than the isomeric furan-1-ones **8** ( $\Delta\delta = 0.15$  ppm). These effects seem to be much smaller for the corresponding DBS forms **11** and **13** (cf. Table 3 and 4).

Dehydrogenation of  $(-)-(P)$ -**5a** led to  $(-)$ -**7a** (cf. Scheme 3) whose CD spectrum is displayed in Fig. 2. It resembles in its long-wavelength part very much the CD spectrum of the starting material  $(-)-(P)$ -**5** (Fig. 1). The CD band at 362 nm of  $(-)-(P)$ -**5** is as expected bathochromically shifted to 392 nm for  $(-)-(P)$ -**7a** due to the strong conjugation with the oxo group of the lactone ring. There is also a strong similarity to the CD spectrum (cyclohexane) of dimethyl  $(-)-(P)$ -5,6,8,10-heptalene-1,2-dicarboxylate which shows its longest-wavelength CD band at 388 nm [10a]. All three compounds, which are linked by the described reduction-dehydrogenation sequence, show in their  $(P)$ -configuration the second negative maximum at 311–318 nm, *i.e.*, this second CE of the inherently chiral heptalene skeleton seems not to be influenced by conjugation.

The CD spectrum of  $(-)-(P)$ -**7a** is also comparable with those of corresponding  $(P)$ -configured 'ortho'-anhydrides of type **2** (cf. [3]) as well as their isomeric forms with the oxo function at  $C(1)$  (cf. [4]).

3.3. *Heptaleno[1,2-c]furans*. The structures of this new type of annelated furans follows clearly from their  $^1H$ -NMR data (cf. Table 5). The fixed C=C bond position of the heptalene skeletons is indicated by the observed vicinal coupling constants of 11.5 Hz between H-C(4) and H-C(5) as well as of 11.8 to 12.0 Hz between H-C(9) and H-C(10) in the case of **6e** and **23e**, respectively. The C=C bond position in **6c** and **6d** is evident from the observed allylic coupling between H-C(4) and  $Me-C(5)$ . Typical for the furan part is the coupling constant of 1.5 Hz between H-C(1) and H-C(3) (cf. [20]). H-C(1) shows also a long-range coupling ( $^5J = 0.7$  Hz) with H-C(4). The other observed couplings are typical for the heptalene skeleton (see *e.g.* [3–5] [10]). The  $^{13}C$ -NMR

Table 3. Chemical Shifts [ppm] and Geminal Coupling Constants [Hz] of the AB System of the CH<sub>2</sub> H-Atoms in the Furan-3-ones **7** and **11**<sup>a)</sup>

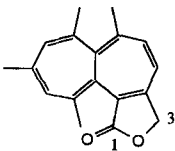
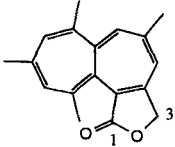
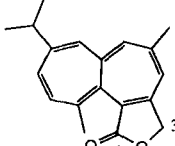
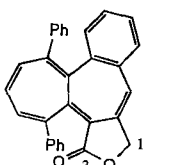
Furan-3-one	$\delta(\text{H}_2\text{C}(1))$		$\Delta\delta(\text{H}_{\text{RS}} - \text{H}_{\text{SR}})$ [ppm]	$^2J(\text{H}_{\text{RS}}, \text{H}_{\text{SR}})$ [Hz]	
	$\text{H}_{\text{RS}}$	$\text{H}_{\text{SR}}$			
	<b>7a</b>	5.11	4.55	0.56	17.7
	<b>7c</b>	5.08	4.54	0.54	17.6
	<b>7d</b>	5.09	4.54	0.55	17.6
	<b>7e</b>	5.12	4.59	0.53	17.8
	<b>11b</b>	4.47	3.93	0.54	13.2
	<b>11d<sup>b)</sup></b>	4.78	4.64	0.14	12.7
	<b>11e<sup>c)</sup></b>	4.76	4.51	0.25	12.8

<sup>a)</sup> In CDCl<sub>3</sub>; see also *Scheme 10*.

<sup>b)</sup> Only observed in traces as a photochemically formed by-product in the CDCl<sub>3</sub> solution of **7d**.

<sup>c)</sup> In thermal equilibrium with 72.5% of **7e** (*cf. Scheme 8*).

Table 4. Chemical Shifts [ppm] and Geminal Coupling Constants [Hz] of the AB System of the CH<sub>2</sub> H-Atoms in the Furan-1-ones **8** and **13**<sup>a)</sup>

Furan-1-one	$\delta(\text{CH}_2(3))$		$\Delta\delta(\text{H}_A - \text{H}_B)$ [ppm]	$^2J(\text{H}_A, \text{H}_B)$ [Hz]
	A	B		
 <b>8a</b>	4.94	4.82	0.12	16.7
 <b>8c</b>	4.84	4.72	0.12	17.0
 <b>8e</b>	4.89	4.74	0.15	16.8
 <b>13b</b> <sup>b)</sup>	5.08	4.93	0.15	13.1

a) In CDCl<sub>3</sub>.

b) Only found in the reaction mixture of the DIBAH reduction of the corresponding benzo[*a*]heptalene-6,7-dicarboxylate **10b** (cf. Scheme 5).

spectrum of **6a** is in full agreement with its proposed structure. This is also true for all measured <sup>1</sup>H-NOE effects (see *Exper. Part*).

The mass spectra (EI, 70 eV) of **6** and **23** show as most intense signal the *M*<sup>+</sup> peak (cf. Table 6). Characteristic is the strong [*M* – 15]<sup>+</sup> peak for most of the furans. This observation speaks for the fact that the *M*<sup>+</sup> ions undergo ring-contraction reactions by cyclization of the *s-cis*-butadiene substructures, followed by loss of Me (cf. Scheme 12). Indeed, the next prominent signals are the [*M* – Me – C≡C – R]<sup>+</sup> peaks (cf. Table 6), arising from the cleavage of the cyclobutene rings. The presence of the furan ring is indicated by the loss of CHO and CH<sub>2</sub>O (cf. [21]).

The heptaleno[1,2-*c*]furans **6a**, **6d**, and **23a** could easily be resolved at room temperature into their (–)-(*P*)- and (+)-(*M*)-antipodes<sup>10)</sup> on an analytical *Chiralcel OD* column

<sup>10)</sup> (*P*) and (*M*) refer to the helicity at the central  $\sigma$  bond (C(6a)–C(11a)) of the heptalene skeleton. See the remarks on the configuration of benzo[*a*]heptalenes and their stereochemical designation in [22] (Footnote 10).

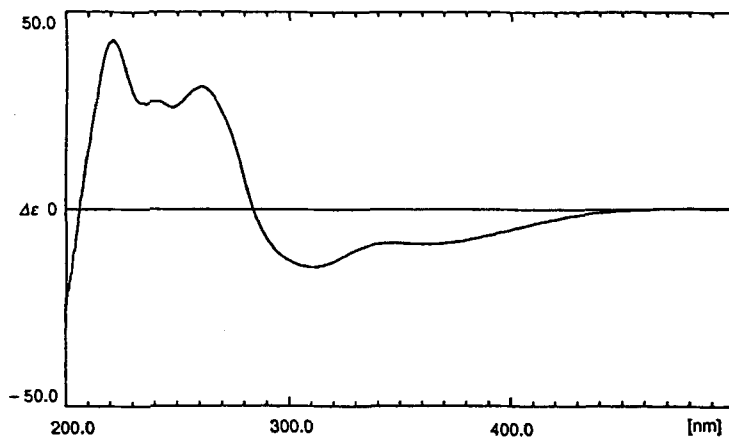


Fig. 1. CD Spectrum (cyclohexane) of  $(-)-(P)$ -5,6,8,10-tetramethylheptalene-1,2-dimethanol ( $(-)-(P)$ -5a)

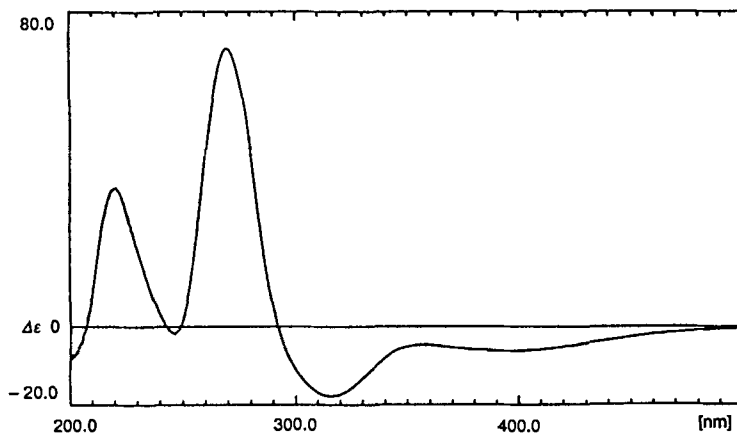
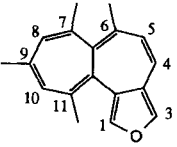
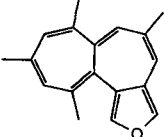
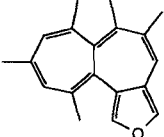
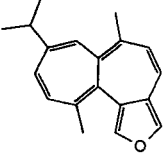
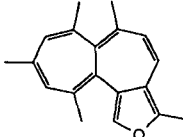
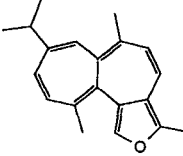


Fig. 2. CD Spectrum (cyclohexane) of  $(-)-(P)$ -1,3-dihydro-6,7,9,11-tetramethylheptaleno[1,2-*c*]furan-3-one ( $(-)-(P)$ -7a)

with hexane as eluant. The remarkable differences in the retention times ( $t_R$ ) of the antipodes ( $t_R((+)-(M)\text{-form})/t_R((-)(P)\text{-form}) = 1.4\text{--}3.0$ ) allowed a complete separation in one run. The CD data of the faster running  $(-)(P)$ -antipodes<sup>11)</sup> are collected in Table 7. There is no doubt on the absolute configuration of the new heptaleno[1,2-*c*]furans **6** and **23**, since  $(-)(P)$ -5a led, upon dehydrogenation with  $\text{MnO}_2$ , to  $(-)(P)$ -6a which exhibited a nearly identical CD spectrum as the faster-moving antipode of **6a** on the *Chiralcel OD* column. Since the  $\Delta\epsilon$  values of both  $(-)$ -6a samples were also identical, we can conclude that no racemization had occurred on the reaction paths of  $(-)(P)$ -5a to

<sup>11)</sup> The antipodes of 1,2,3,9,10-pentamethoxybenzo[*a*]heptalenes show on the same analytical *Chiralcel OD* column with hexane/*i*-PrOH (85–95%/15–5%) as eluant a similar retention-time behavior, i.e.,  $t_R((+)-(M)\text{-forms})/t_R((-)(P)\text{-forms}) = 1.2\text{--}1.4$  (cf. [22]).

Table 5. <sup>1</sup>H-NMR Data [CDCl<sub>3</sub>] of the Heptaleno[1,2-*c*]furans **6** and **23**<sup>a)</sup>

Furan	H-C(1)	R-C(3)	H-C(4)	R-C(5)	R-C(6)	R-C(7)	R-C(8) b)	R-C(9)	H-C(10) c)	Me-C(11)
	<b>6a</b> 7.12 ( <i>dd</i> , <i>J</i> = 1.5, 0.7)	7.45 ( <i>d</i> , <i>J</i> = 1.5)	6.58 ( <i>d</i> , <i>J</i> = 11.5)	5.95 ( <i>d</i> , <i>J</i> = 11.5)	1.74 ( <i>s</i> )	1.96 ( <i>d</i> , <i>J</i> = 1.3)	6.08 ( <i>s</i> )	2.00 ( <i>d</i> , <i>J</i> = 1.2)	6.12 ( <i>s</i> )	1.85 ( <i>s</i> )
	<b>6c</b> 7.11 ( <i>dd</i> , <i>J</i> = 1.5, 0.7)	7.35 ( <i>d</i> , <i>J</i> = 1.5)	6.37 ( <i>qd</i> , <i>J</i> = 1.5, 0.7)	1.92 ( <i>d</i> , <i>J</i> = 1.4)	5.53 ( <i>s</i> )	2.08 ( <i>d</i> , <i>J</i> = 1.1)	5.94 ( <i>s</i> )	1.96 ( <i>d</i> , <i>J</i> = 1.3)	6.08 ( <i>s</i> )	1.87 ( <i>s</i> )
	<b>6d</b> 7.09 ( <i>dd</i> , <i>J</i> = 1.4, 0.8)	7.39 ( <i>d</i> , <i>J</i> = 1.2)	6.50 ( <i>s</i> ) <sup>d)</sup>	1.98 ( <i>d</i> , <i>J</i> = 1.3)	1.75 ( <i>s</i> )	1.95 ( <i>d</i> , <i>J</i> = 1.2)	6.00 ( <i>s</i> )	2.01 ( <i>d</i> , <i>J</i> = 1.0)	6.11 ( <i>s</i> )	1.85 ( <i>s</i> )
	<b>6e</b> 7.16 ( <i>dd</i> , <i>J</i> = 1.5, 0.7)	7.41 ( <i>d</i> , <i>J</i> = 1.5)	6.55 ( <i>d</i> , <i>J</i> = 11.5)	5.96 ( <i>d</i> , <i>J</i> = 11.5)	1.74 ( <i>d</i> , <i>J</i> = 0.9)	5.69 ( <i>s</i> ) <sup>e)</sup>	2.54 ( <i>sept. d</i> , <i>J</i> = 6.9, 0.6); 1.15; 1.13 ( <i>d</i> , <i>J</i> = 6.9, 6.8)	6.33 ( <i>dd</i> , <i>J</i> = 12, 1.3)	6.34 ( <i>d</i> , <i>J</i> = 12.2)	1.89 ( <i>s</i> )
	<b>23a</b> 6.99 ( <i>s</i> )	2.33 ( <i>s</i> )	6.49 ( <i>d</i> , <i>J</i> = 11.5)	5.90 ( <i>d</i> , <i>J</i> = 11.5)	1.74 ( <i>s</i> )	1.96 ( <i>d</i> , <i>J</i> = 1.3)	6.08 ( <i>s</i> )	2.00 ( <i>d</i> , <i>J</i> = 1.2)	6.12 ( <i>s</i> )	1.87 ( <i>s</i> )
	<b>23e</b> 7.02 ( <i>s</i> )	2.30 ( <i>s</i> )	6.45 ( <i>d</i> , <i>J</i> = 11.5)	5.89 ( <i>d</i> , <i>J</i> = 11.5)	1.73 ( <i>d</i> , <i>J</i> = 1.0)	5.68 ( <i>s</i> ) <sup>e)</sup>	2.53 ( <i>sept. d</i> , <i>J</i> = 6.8, 0.5); 1.14; 1.12 ( <i>d</i> , <i>J</i> = 6.9, 6.8)	6.29 ( <i>dd</i> , <i>J</i> = 11.8, 1.4)	6.33 ( <i>dd</i> , <i>J</i> = 11.8, 0.5)	1.89 ( <i>s</i> )

a) Chemical shifts in ppm; *J* in Hz; R = H, Me, or *i*-Pr.

b) H-C(8) appears in most cases as *quint.*-like due to  ${}^4J(\text{Me-C}(7), \text{H-C}(8)) \approx {}^4J(\text{H-C}(10), \text{H-C}(8)) \approx 1.3$ .

c) H-C(10) appears as broad *s* due to  ${}^4J(\text{Me-C}(9), \text{H-C}(10)) \approx {}^4J(\text{H-C}(8), \text{H-C}(10))$ .

d) H-C(4) appears as broad *s* due to  ${}^4J(\text{Me-C}(5), \text{H-C}(4)) \approx 2 \cdot {}^5J(\text{H-C}(1), \text{H-C}(4))$ .

e) H-C(7) appears as broad *s* due to  ${}^5J(\text{Me-C}(6), \text{H-C}(7)) \approx {}^4J(\text{Me}_2\text{CH-C}(8), \text{H-C}(7)) \approx {}^4J(\text{H-C}(9), \text{H-C}(7))$ .



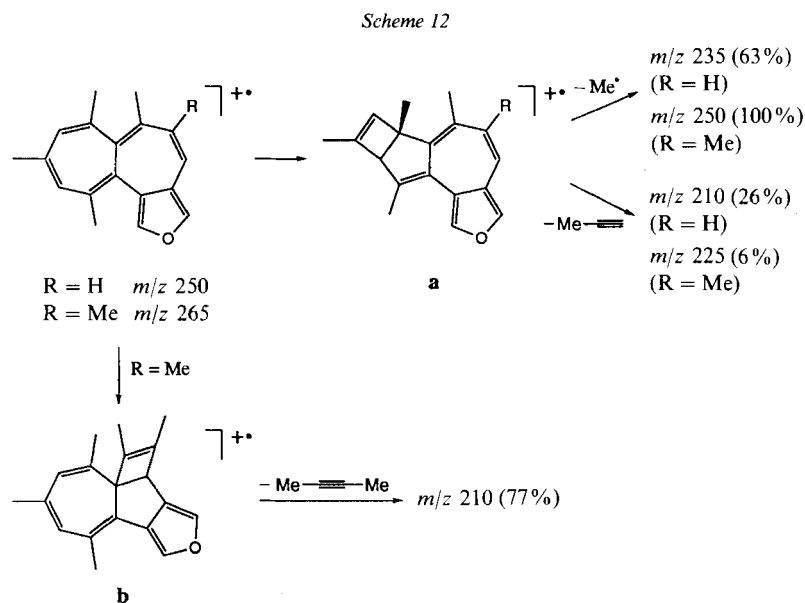
Table 6. Characteristic Fragment-Ion Peaks in the Mass Spectra of the Heptaleno[1,2-c]furans **6** and **23a**<sup>a)</sup>

Heptaleno-furan	$M^+$	$[M - \text{Me}]^+$	$[M - \text{CHO}]^+$	$[M - \text{CH}_2\text{O}]^+$	$[M - \text{Me} - \text{C}\equiv\text{CH}]^+$	$[M - \text{Me} - \text{C}\equiv\text{C} - \text{Me}]^+$
<b>6a</b>	100	63	6	14	26	–
<b>6c</b>	100	26	5	5	5	–
<b>6d</b>	91	100	8	23	6	77
<b>6e</b>	100	19(17) <sup>b)</sup>	2	4	15(17) <sup>c)</sup>	–
<b>23a</b>	100	41	5	11	21	–
<b>23e</b>	100	13(8) <sup>b)</sup>	1	3	6(8) <sup>c)</sup>	–

a) Relative %.

b) In parentheses,  $[M - i\text{-Pr}]^+$  and/or  $[M - \text{MeCO}]^+$ .

c) In parentheses,  $[M - i\text{-Pr} - \text{C}\equiv\text{CH}]^+$ .


 Table 7. CD Data (hexane) of the Heptaleno[1,2-c]furans **6a**, **6d**, and **23a**<sup>a)</sup>

Heptaleno-furan	$t_R(M)/t_R(P)^b$	Cotton effect				
		1	2	3	4	5
(-)-(P)- <b>6a</b> <sup>c)</sup>	1.4	320 (-25.0)	297 (sh, -19.7)	257 (sh, 14.3)	233 (sh, 71.0)	223 (87.3)
		321 (-26.9)	297 (sh, -20.5)	258 (sh, 15.1)	233 (sh, 76.6)	223 (93.0)
(-)-P- <b>6d</b>	1.4		313 (-29.9)	260 (sh, 9.6)	235 (90.1)	230 (sh, 87.1)
(-)-P- <b>23a</b>	3.0		318 (-32.6)	257 (sh, 17.7)	236 (76.8)	227 (sh, 73.8)

a) Data in nm ( $\Delta\epsilon$ ); for (+)-(M)-antipodes, see *Exper. Part*.

b) Retention-time ratio on the analytical *Chiralcel OD* column (see *Exper. Part*) of the antipodes.

c) Second line: (-)-(P)-**6a** from the dehydrogenation reaction of (-)-(P)-**5a** with  $\text{MnO}_2/\text{CH}_2\text{Cl}_2$ .

(-)-(P)-**6a** in the  $\text{MnO}_2$  reaction (*cf. Scheme 7*). Indeed, the optical isomers of **6a** and **6d** turned out to be optically quite stable. The racemization of both heptaleno[1,2-*c*]furans at  $120^\circ$  in heptane, followed by the decrease of  $\Delta\epsilon$  of the most intense CD band (*cf. Table 7*), obeyed first-order kinetics with  $\tau_{1/2} = 178$  min for **6a** and 207 min for **6d**, *i.e.*,  $k_{\text{rac}}(\mathbf{6d})/k_{\text{rac}}(\mathbf{6a}) = 1.16$ . The by 16% higher optical stability of **6d** as compared with **6a** can be attributed to the buttressing effect of Me-C(5) in **6d**, which is not present in **6a**.

The CD spectra of all three resolved heptaleno[1,2-*c*]furans are displayed in *Fig. 3–5*. As can be seen, there are slight changes in the CD spectra in going from **6a** to **6d** and **23a**. Whereas **6a** exhibits two CD bands in the long-wavelength region, one clearly visible at 320–321 nm and the other as a shoulder at 297 nm, there is only one CD band detectable in the spectra of **6d** (314 nm) and **23a** (318 nm). The habitus of the CD band of **6d** is still

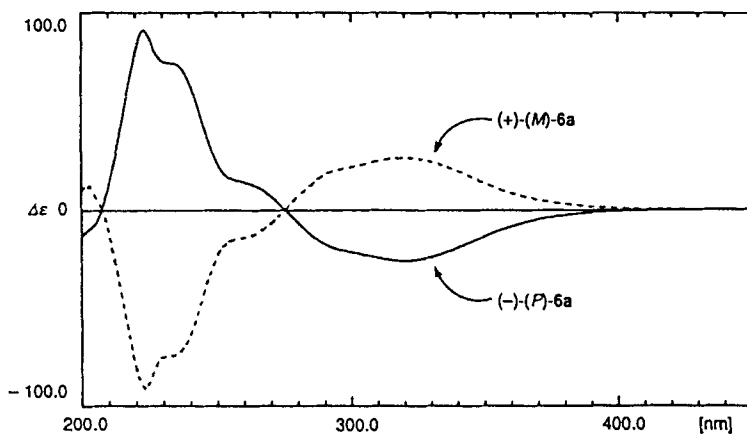


Fig. 3. CD Spectra (hexane) of (-)-(P)- and (+)-(M)-6,7,9,11-tetramethylheptaleno[1,2-*c*]furan ((-)-(P)-**6a** and (+)-(M)-**6a**)

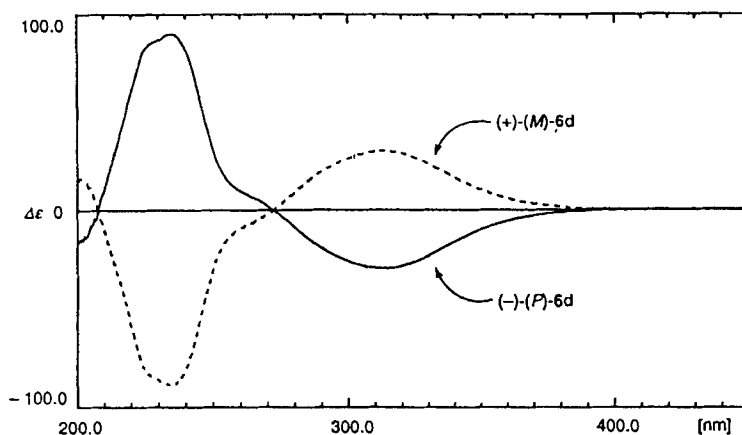


Fig. 4. CD Spectra (hexane) of (-)-(P)- and (+)-(M)-5,6,7,9,11-pentamethylheptaleno[1,2-*c*]furan ((-)-(P)-**6d** and (+)-(M)-**6d**)

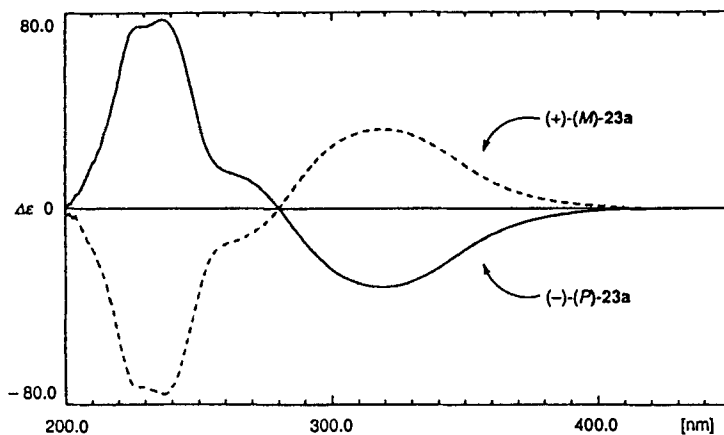


Fig. 5. CD Spectra (hexane) of  $(-)-(P)$ - and  $(+)-(M)$ -3,6,7,9,11-pentamethylhepteno[1,2-*c*]furan ( $(-)-(P)$ -**23a** and  $(+)-(M)$ -**23a**)

slightly asymmetric with a faint indication of a shoulder around 290 nm (*cf.* Fig. 4). We interpret these observations as the result of a higher degree of twisting of the heptalene skeleton of **6d** and presumably also of **23a** compared with **6a**.

The twisting effects of the heptalene skeleton are also reflected in the UV spectra of **6** and **23** (Table 8 and Figs. 6–9). The long-wavelength band of **6a** is just resolved and appears in perfect agreement with the CD spectrum at 319 nm. The second CD band of **6a**, which appears as a shoulder at 297 nm, is not recognizable in the UV spectrum, because it is completely covered by the intense UV absorption band at 278 nm. The heptalene absorption band of **6d** appears in the UV spectrum only as a shoulder at 314 nm and is followed by the intense second UV absorption band at 273 nm. Still less developed is the heptalene absorption band in the UV spectrum of **23d**. It appears as a shoulder at 324 nm on the second absorption band at 282 nm, *i.e.*, its real position is better reflected in CD band at 318 nm. That the degree of twisting is the main reason for the shifts in the long-wavelength heptalene absorption band can be realized by taking into account the UV data of **6c**. It is a positional isomer of **6a**, however, with one free *peri*-position (C(6)).

Table 8. UV Absorption Bands ( $\lambda_{\max}$  [nm] (log  $\epsilon$ ; hexane) of the Heptaleno[1,2-*c*]furans **6** and **23a**<sup>a)</sup>

Heptaleno-furan	1	2	3	4	5
<b>6a</b>	319.2 (3.69)	275.6 (4.12)	233.6 (sh, 4.18)	218.4 (4.35)	– <sup>b)</sup>
<b>6c</b>	334.4 (3.75)	278.0 (4.08)	238.8 (sh, 4.12)	–	–
<b>6d</b>	314 (sh, 3.76)	273.2 (4.19)	ca. 240 (sh, 4.2)	215.6 (4.42)	–
<b>6e</b>	324.8 (4.02)	282.8 (4.47)	237.2 (sh, 4.44)	213.6 (sh, 4.70)	204.4 (4.70)
<b>23a</b>	324 (sh, 3.77)	282.4 (4.15)	ca. 240 (sh, 4.2)	220.8 (4.40)	–
<b>23e</b>	331 (sh, 3.78)	290.0 (4.16)	239.2 (sh, 4.13)	210.4 (4.40)	–

<sup>a)</sup> For  $\lambda_{\min}$ , see *Exper. Part*.

<sup>b)</sup> – = Not recorded.

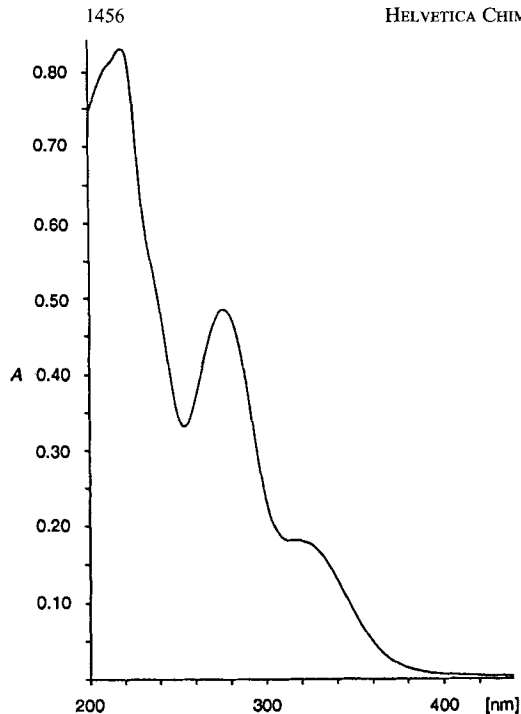


Fig. 6. UV Spectrum (hexane) of 6,7,9,11-tetramethylheptaleno[1,2-c]furan (6a)

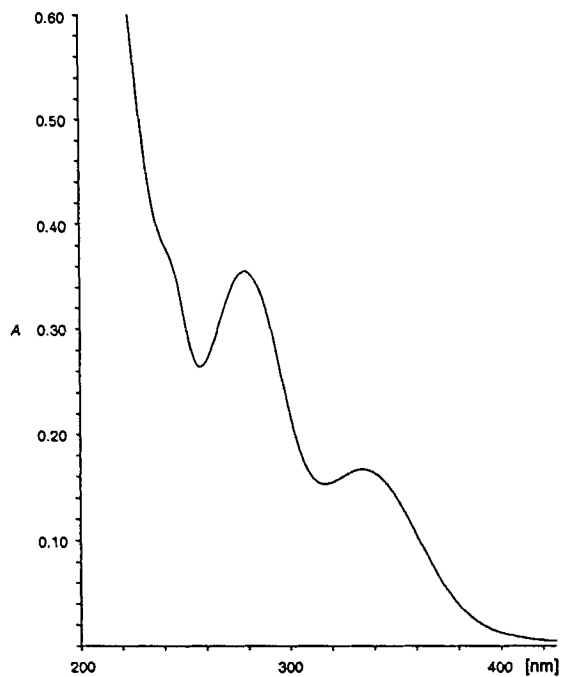


Fig. 7. UV Spectrum (hexane) of 5,7,9,11-tetramethylheptaleno[1,2-c]furan (6c)

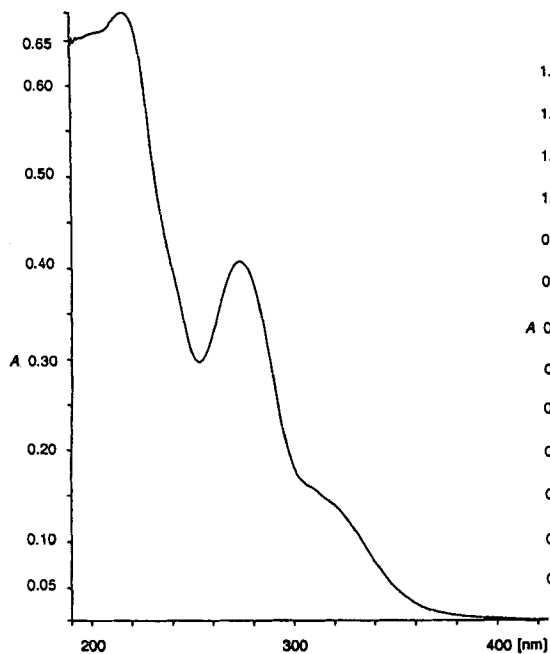


Fig. 8. UV Spectrum (hexane) of 5,6,7,9,11-pentamethylheptaleno[1,2-c]furan (6d)

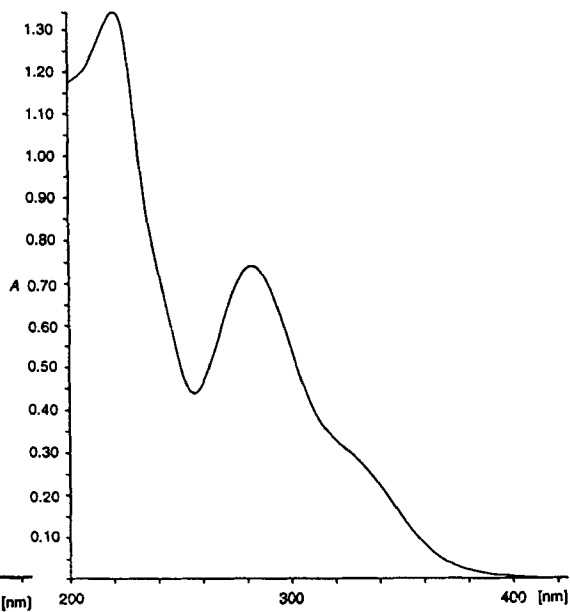


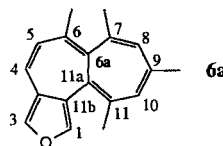
Fig. 9. UV Spectrum (hexane) of 3,6,7,9,11-pentamethylheptaleno[1,2-c]furan (23a)

It shows a well-developed heptalene absorption band at 334 nm<sup>12</sup>). It is bathochromically shifted by 15 nm as compared with **6a**. We observed a similar shift effect of the heptalene absorption band in the CD spectra of 1,2,3,9,10-pentamethoxybenzo[*a*]heptalene and its 4-methyl derivative [22]. The X-ray crystal-structure analysis of both compounds revealed an increase of the central heptalene *gauche* angles from at least 52 to 59°, accompanied by a hypsochromic shift of the heptalene absorption band by 12 nm [22], *i.e.*, the *peri*-positioned Me group at C(4) of the benzo[*a*]heptalene skeleton has a significant influence on the twisting of the heptalene skeleton.

The Me substituent at C(4) of the benzo[*a*]heptalenes can be compared with the Me substituent at C(3) of **23a**. However, the different valence angles of the benzo and the furano ring cause less steric hindrance in **23a** as compared with the benzo[*a*]heptalenes. Indeed, the heptalene CD band of **6a** and **23a** shows only marginal differences. The difference is larger and goes in an opposite direction in the UV spectra. However, the UV spectrum of **23a** shows the heptalene absorption band only as a badly resolved shoulder (*cf.* Fig. 9), which allows no clear assignment of the position.

Unfortunately, the quality of the crystals of the heptaleno[1,2-*c*]furans, which are extremely soluble already in hexane, allowed so far no X-ray crystal-structure determination. However, MM2 calculations are in agreement with our observations. Table 9 contains the calculated main torsional angles of **6a**, **6c**, **6d**, and **23a**. The average value of the central heptalene *gauche* angles (Entry 14) increases indeed in the sequence **6c**, **6a** (**23a**), and **6d**. This order is also reflected in the average value of the torison angles of the

Table 9. Calculated Torsion Angles ( $\theta$ ) of the Skeleton of the Heptaleno[1,2-*c*]furans **6a**, **6c**, **6d**, and **23a**<sup>a)</sup>



Entry	$\theta$ [°]	<b>6a</b>	<b>6c</b>	<b>6d</b>	<b>23a</b>
1	C(3)–C(3a)–C(4)–C(5)	–157.7	–158.9	–158.9	–156.3
2	C(4)–C(5)–C(6)–C(6a)	–34.4	–32.8	–38.6	–34.0
3	C(6)–C(6a)–C(7)–C(8)	119.2	125.1	117.2	119.2
4	C(7)–C(8)–C(9)–C(10)	35.8	32.5	37.0	35.7
5	C(9)–C(10)–C(11)–C(11a)	–33.7	–30.6	–34.6	–33.5
6	C(11)–C(11a)–C(11b)–C(1)	–50.4	–47.4	–49.8	–51.3
7	C(11a)–C(11b)–C(3a)–C(4)	–2.2	–2.6	–5.6	–2.6
8	C(11b)–C(3a)–C(4)–C(5)	29.3	27.1	31.4	30.7
9	C(6)–C(6a)–C(11a)–C(11b)	53.6	50.8	57.2	54.0
10	C(7)–C(6a)–C(11a)–C(11)	58.9	53.9	60.0	58.6
11	C(6)–C(6a)–C(11a)–C(11)	–124.3	–128.4	–122.6	–124.3
12	C(7)–C(6a)–C(11a)–C(11b)	–123.2	–126.9	–120.3	–123.1
13	$\theta_{av}(2, 4, 5, 8)^b$	33.3	30.8	35.4	33.5
14	$\theta_{av}(9, 10)^c$	56.3	52.4	58.6	56.3

<sup>a)</sup> MM2 calculated torsion angles for the (*P*)-configuration.

<sup>b)</sup>  $\theta_{av}$  = average torsion angle of the *s-cis*-butadiene subunits (Entries 2, 4, 5, and 8).

<sup>c)</sup>  $\theta_{av}$  = average *gauche* torsion angle at the central heptalene bond (Entries 9, and 10).

<sup>12)</sup> Neither **6c** nor **6e** could be resolved into their antipodes on the analytical *Chiralcel OD* column with hexane as eluant.

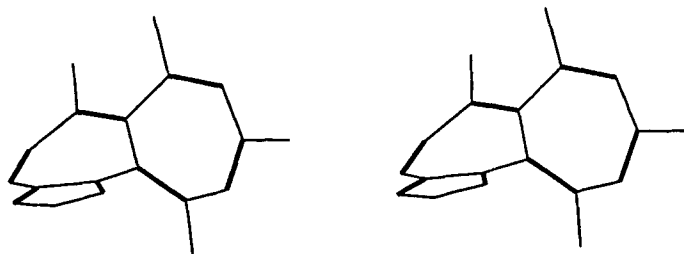


Fig. 10. Stereoprojection of the calculated structure of (*M*)-6,7,9,11-tetramethylheptaleno[1,2-*c*]furan ((*M*)-**6a**); only the positions of the C-atoms are shown. The O-atom in position 2 is not especially indicated

*s-cis*-butadiene subunits of the heptalene skeleton (*Entry 13*). The Me group at C(3) in **23a** does not change very much indeed these average values as compared with **6a**, in contrast to the effects in benzo[*a*]heptalenes. Therefore, there is little doubt that the UV absorptions and their CD effects from 290 nm on have to be attributed to the globally C<sub>2</sub>-twisted heptalene skeleton (*cf. Fig. 10*).

We thank Prof. *M. Hesse* and his coworkers for mass spectra, Prof. *W. von Philipsborn* and his coworkers for NMR support and numerous <sup>1</sup>H-NOE measurements, as well as Dr. *R. W. Kunz* for MM2 calculations, and *J. Kessler* and *H. Frohofer* for elemental analyses. Technical assistance by *Leonidas Agorastos* and financial support by the *Swiss National Science Foundation* is gratefully acknowledged.

### Experimental Part

*General.* See [1] [15]. CD data in *Ae*.

**1. Heptalene-4,5-4 and Heptalene-1,2-dimethanols 5 by Reduction of Dimethyl Heptalene-dicarboxylates 10 with DIBAH or LiAlH<sub>4</sub>.** – 1.1. *1,6,8,10-Tetramethylheptalene-4,5-dimethanol (4a)*. See [1] as well as *Table 2*.

1.1.1. *5,6,8,10-Tetramethylheptalene-1,2-dimethanol (5a)*<sup>13</sup>. The corresponding dimethyl heptalene-1,2-dicarboxylate (9.3 g, 28.5 mmol) [10a], dissolved in Et<sub>2</sub>O (250 ml), was added dropwise to an ice-cooled soln. of LiAlH<sub>4</sub> (2.9 g, 76.4 mmol) in Et<sub>2</sub>O (70 ml). The temp. of the mixture was kept in the range of 5–10°. After the addition of the diester, the mixture was stirred during 5 h at r.t. and then decomposed under ice-cooling with H<sub>2</sub>O (10 ml) and 1N HCl (200 ml). The aq. phase was extracted with Et<sub>2</sub>O, and the combined Et<sub>2</sub>O phases were washed with H<sub>2</sub>O. The product was crystallized after the removal of Et<sub>2</sub>O and recrystallized from Et<sub>2</sub>O. M.p. 135–136°. *R<sub>f</sub>* (Et<sub>2</sub>O) 0.43. UV (cyclohexane): λ<sub>max</sub> 355 (sh with tailing, 2.75), 299 (sh, 348), 257 (4.34), 214 (4.22); λ<sub>min</sub> 230 (4.02). IR (KBr): 3390 (OH), 2965, 2938, 2912, 2856, 2725, 1645, 1609, 1519, 1440, 1372, 1197, 1166, 1116, 1084, 1026, 997, 845, 790, 747. <sup>1</sup>H-NMR (270 MHz, CDCl<sub>3</sub>)<sup>14</sup>: 6.405 (*AB*, slightly resolved, *J*<sub>*AB*</sub> = 11.8, H–C(3,4)); 6.108 (br. *s*, H–C(9)); 6.012 (br. *s*, H–C(7)); 4.594, 4.090 (*AB*, *J*<sub>*AB*</sub> = 12.9, HOCH<sub>2</sub>–C(1)); 4.502, 4.275 (*AB*, *J*<sub>*AB*</sub> = 12.0, HOCH<sub>2</sub>–C(2)); 2.20 (br. *s*, 2 OH); 2.008 (*d*-like <sup>4</sup>*J*(H–C(7), Me–C(6)) = 1.3, Me–C(6)); 1.992 (*d*-like, <sup>4</sup>*J*(H–C(9), Me–C(8)) = 1.2, Me–C(8)); 1.759 (*s*, Me–C(5)); 1.654 (*s*, Me–C(10)). <sup>13</sup>C-NMR (100 MHz, CDCl<sub>3</sub>): 138.12 (*q*-like, <sup>2</sup>*J*(Me–C(8)) = 6.1, C(8)); 138.04 (*t*-like, C(1)); 136.29 (br. *s*, C(5a)); 135.78 (*dq*-like, <sup>1</sup>*J* = 155, <sup>3</sup>*J*(Me–C(5)) = 3.8, C(4)); 134.76 (br. *s*, C(2)); 133.10 (*q*, <sup>2</sup>*J*(Me–C(6)) = 6.3, C(6)); 132.00 (*dt*-like, <sup>1</sup>*J* = 155, <sup>3</sup>*J*(HOCH<sub>2</sub>–C(2)) = 4.5, C(3)); 130.43 (*dsext*-like, <sup>1</sup>*J* = 152, <sup>3</sup>*J*(Me–C(8)) ≈ <sup>3</sup>*J*(H–C(7)) = 5.5, C(9)); 129.85 (br. *s*, C(10a)); 129.51 (*dsept*-like, <sup>1</sup>*J* = 150, <sup>3</sup>*J*(Me–C(6)) ≈ <sup>3</sup>*J*(Me–C(8)) ≈ <sup>3</sup>*J*(H–C(9)) = 5.0, C(7)); 128.77 (*q*-like, <sup>2</sup>*J*(Me–C(10)) = 5.5, C(10)); 127.49 (*dq*-like, <sup>3</sup>*J*(H–C(3)) = 11.6, <sup>2</sup>*J*(Me–C(5)) = 5.9, C(5)); 63.36 (*t*, <sup>1</sup>*J* = 143, HOCH<sub>2</sub>–C(1)); 62.88 (*t*, <sup>1</sup>*J* = 143, HOCH<sub>2</sub>–C(2)); 25.07 (*qdd*, <sup>1</sup>*J* = 126, <sup>3</sup>*J*(H–C(9)) = 7.0, <sup>3</sup>*J*(H–C(7)) = 3.3, Me–C(8)); 23.11 (*qd*, <sup>1</sup>*J* = 127, <sup>3</sup>*J*(H–C(7)) = 6.1, Me–C(6)); 17.69 (*qd*, <sup>1</sup>*J* = 127, <sup>3</sup>*J*(H–C(4)) = 3.8, Me–C(5)); 17.66 (*qd*, <sup>1</sup>*J* = 127, Me–C(10)). MS: Identical with that of **4a** [1]. Anal. calc. for C<sub>18</sub>H<sub>22</sub>O<sub>2</sub> (270.37): C 79.96, H 8.20; found: C 79.68, H 8.52.

<sup>13</sup>) Data from [12].

<sup>14</sup>) Assignments according to the <sup>1</sup>H, <sup>13</sup>C-correlation spectrum.

1.1.2. (–)-(P)-5,6,8,10-Tetramethylheptalene-1,2-dimethanol ((–)-(P)-5a). Optically pure dimethyl (–)-(P)-5,6,8,10-tetramethylheptalene-1,2-dicarboxylate (0.63 g, 1.90 mmol) [10a] was reduced with  $\text{LiAlH}_4$  in  $\text{Et}_2\text{O}$ . The crystallization from  $\text{Et}_2\text{O}$  gave in a first crop (0.072 g, 14%) optically pure (–)-(P)-5a. M.p. 125–127°. CD (cyclohexane; cf; Fig. 1): 365 (–8.0), 344 (–8.0), 311 (–14.85), 283 (0), 269 (sh, 23.7), 261 (31.26), 247 (25.83), 242 (27.66), 235 (27.00), 221 (43.05), 206 (0).

1.2. 8,12-Diphenylbenzo[*a*]heptalene-6,7-dimethanol (4b). Heptalene-dicarboxylate 10b (1.138 g, 2.41 mmol) [13] was dissolved in THF (75 ml, dist. over K) and cooled to 0°. DIBAH (24.5 ml of a 20% soln. in hexane; 24.1 mmol) was added dropwise within 20 min under stirring. Stirring was continued for 2 h.  $\text{H}_2\text{O}$  (10 ml) and then  $\text{AcOEt}$  (100 ml) was added and the org. phase extracted with 2N  $\text{H}_2\text{SO}_4$  (3 × 50 ml). The org. phase was washed with sat. NaCl soln. (50 ml) and dried ( $\text{MgSO}_4$ ). The solvent mixture was evaporated and the residue subjected to CC (silica gel;  $\text{Et}_2\text{O}$ /hexane 4:1). The products were eluted in the order 13b (0.030 g, 3%), 12 (0.045 g, 4.2%), and 4b (0.896 g, 89%).

1,3-Dihydro-9,13-diphenylbenzo[1,2]heptaleno[4,5-*c*]furan-1-one (13b): Orange crystals from  $\text{Et}_2\text{O}$ /hexane. M.p. 203.3–204.8°.  $R_f$  ( $\text{Et}_2\text{O}$ /hexane 1:1): 0.24. UV (hexane):  $\lambda_{\text{max}}$  376 (3.62), 272 (4.40), 259 (4.40); 222 (sh, 4.54);  $\lambda_{\text{min}}$  351 (3.56), 267 (4.40), 252 (4.40). IR (KBr): 3442w, 3053w, 3019w, 2928w, 2880w, 1756s, 1637m, 1596w, 1582w, 1492w, 1470w, 1444w, 1346m, 1230w, 1193w, 1155s, 1076m, 1067m, 1023m, 781m, 756m, 744m, 703m, 688m.  $^1\text{H-NMR}$  (300 MHz,  $\text{CDCl}_3$ ): 7.37 (dd,  $^3J(5,6) = 7.7$ ,  $^4J(5,7) = 1.1$ , H–C(5)); 7.34–7.31 (m, 2 arom. H); 7.28 (td,  $^3J(6,7/5,6) = 7.7$ ,  $^4J(6,8) = 1.2$ , H–C(6)); 7.20 (td,  $^3J(7,8/6,7) = 7.4$ ,  $^4J(5,7) = 1.4$ , H–C(7)); 7.19–7.09 (m, 3 arom. H); 7.08–6.90 (m, 3 arom. H, H–C(12), H–C(4)); 6.86–6.78 (m, 2 arom. H, H–C(11)); 6.66 (d,  $^3J(10,11) = 11.6$ , H–C(10)); 6.65 (dd,  $^3J(7,8) = 7.8$ ,  $^4J(6,8) = 1.3$ , H–C(8)); 5.08, 4.93 (ABX,  $^2J_{AB} = 13.1$ ,  $^4J_{AX} = ^4J(3,4) = 1.9$ ,  $^4J_{BX} = ^4J(3,4) = 1.5$ ,  $\text{H}_2\text{C}(3)$ ).  $^{13}\text{C-NMR}$  (75 MHz,  $\text{CDCl}_3$ ): 166.24 (C(1)); 143.88 (C(13a)); 140.78 (C(9 or 13)); 140.76 (1 arom. C); 139.63 (1 arom. C); 137.71 (C(4a)); 136.67 (C(9 or 13)); 135.84 (C(3a)); 134.11 (C(10)); 131.97 (C(11)); 131.59 (C(8a)); 131.52 (C(7)); 130.89 (C(8b)); 130.74 (C(8)); 130.09 (2 arom. C); 128.81 (C(5)); 128.29 (2 arom. C); 127.78 (C(6), C(12)); 127.70 (2 arom. C); 127.27 (C(4)); 127.22 (1 arom. C); 126.88 (3 arom. C); 121.76 (C(13b)); 69.52 (C(3)). CI-MS ( $\text{NH}_3$ ): 430 (6,  $[\text{M} + \text{NH}_4]^+$ ), 413 (51,  $[\text{M} + 1]^+$ ), 412 (100,  $\text{M}^+$ ). EI-MS: 413 (34,  $[\text{M} + 1]^+$ ), 412 (100,  $\text{M}^+$ ), 368 (11,  $[\text{M} - \text{CO}_2]^+$ ), 367 (13,  $[\text{M} - \text{CO}_2 - 1]^+$ ), 310 (38,  $[\text{M} - \text{PhC}\equiv\text{CH}]^+$ ), 234 (24,  $[\text{M} - \text{C}_6\text{H}_4 - \text{PhC}\equiv\text{CH}]^+$ ). Anal. calc. for  $\text{C}_{30}\text{H}_{20}\text{O}_2$  (412.49): C 87.36, H 4.89; found: C 87.66, H 5.12.

Methyl 6-(Hydroxymethyl)-8,12-diphenylbenzo[*a*]heptalene-7-carboxylate (12): Yellow crystals from  $\text{Et}_2\text{O}$ /hexane. M.p. 155–167°.  $R_f$  ( $\text{Et}_2\text{O}$ /hexane 5:1): 0.27.  $^1\text{H-NMR}$  (300 MHz,  $\text{CDCl}_3$ ): 7.56 (s, H–C(5)); 7.41 (d, with f.s.,  $^3J(3,4) = 7.1$ , H–C(4)); 7.25 (td,  $^3J(2,3/3,4) = 7.5$ ,  $^4J(1,3) = 1.2$ , H–C(3)); 7.20–7.03 (m, 8 arom. H, H–C(2)); 6.91 (dd,  $^3J(9,10) = 6.4$ ,  $^4J(9,11) = 0.9$ , H–C(9)); 6.88–6.75 (m, 2 arom. H); 6.86 (dd,  $^3J(9,10) = 6.4$ ,  $^3J(10,11) = 11.0$ , H–C(10)); 6.70 (dd,  $^3J(10,11) = 11.0$ ,  $^4J(9,11) = 0.9$ , H–C(11)); 6.58 (d, with f.s.,  $^3J(1,2) = 7.4$ , H–C(1)); 4.44 (ddd, A of ABXY,  $^2J_{AB} = 13.1$ ,  $^3J_{AX} = ^3J(\text{HOCH}_A\text{H}_B - \text{C}(6)) = 8.7$ ,  $^4J_{AY} = ^4J(5, \text{HOCH}_A\text{H}_B - \text{C}(6)) = 1.0$ ,  $\text{HOCH}_A\text{H}_B - \text{C}(6)$ ); 4.23 (dd, B of ABXY,  $^2J_{AB} = 13.1$ ,  $^3J_{BX} = ^3J(\text{HOCH}_A\text{H}_B - \text{C}(6)) = 3.9$ ,  $^4J_{BY} = ^4J(5, \text{HOCH}_A\text{H}_B - \text{C}(6)) = 0$ ,  $\text{HOCH}_A\text{H}_B - \text{C}(6)$ ); 3.25 (s, MeOCO), 2.22 (dd,  $^3J(\text{HOCH}_A\text{H}_B - \text{C}(6)) = 8.7$ ,  $^3J(\text{HOCH}_A\text{H}_B - \text{C}(6)) = 4.6$ , OH). EI-MS: 444 (25,  $\text{M}^+$ ), 427 (30,  $[\text{M} - \text{OH}]^+$ ), 426 (100,  $[\text{M} - \text{H}_2\text{O}]^+$ ), 413 (16,  $[\text{M} - \text{CH}_2\text{OH}]^+$ ), 412 (43,  $[\text{M} - \text{CH}_2\text{OH}]^+$ ), 368 (28,  $[\text{M} - \text{OH} - \text{OCOCH}_3]^+$ ), 367 (74,  $[\text{M} - \text{H}_2\text{O} - \text{OCOCH}_3]^+$ ), 330 (58,  $[\text{M} - \text{HOCH}_2\text{C}\equiv\text{CCOOH}_3]^+$ ), 310 (21,  $[\text{M} - \text{PhC}\equiv\text{CH} - \text{CH}_2\text{OH}]^+$ ), 289 (26,  $[\text{M} - \text{C}_6\text{H}_6 - \text{Ph}]^+$ ), 252 (30,  $[\text{M} - \text{C}_6\text{H}_6 - \text{HOCH}_2\text{C}\equiv\text{CCOOCH}_3]^+$ ).

Data of 4b. Yellow foam, which crystallized after treatment with  $\text{Et}_2\text{O}$ /hexane. M.p. 83–119°.  $R_f$  ( $\text{Et}_2\text{O}$ /hexane 5:1): 0.23. UV (hexane):  $\lambda_{\text{max}}$  335 (sh, 3.56); 279 (4.39); 229 (sh, 4.44);  $\lambda_{\text{min}}$  256 (4.28). IR (KBr): 3386s, 3055m, 3018m, 2955m, 2924m, 2871w, 1596w, 1491m, 1480w, 1443m, 1023s, 797w, 755s, 719m, 700s, 607w, 566w, 518w.  $^1\text{H-NMR}$  (300 MHz,  $\text{CDCl}_3$ ): 7.42 (d, with f.s.,  $^3J(3,4) = 7.5$ , H–C(4)); 7.39 (s, H–C(5)); 7.29–7.21 (m, 2 arom. H, H–C(3)); 7.18–7.11 (m, 3 arom. H); 7.09–7.01 (m, 3 arom. H, H–C(2)); 6.95 (d,  $^3J(9,10) = 6.0$ , H–C(9)); 6.86–6.82 (m, 2 arom. H); 6.77 (dd,  $^3J(9,10) = 6.1$ ,  $^3J(10,11) = 11.5$ , H–C(10)); 6.63 (d,  $^3J(10,11) = 11.4$ , H–C(11)); 6.56 (d, with f.s.,  $^3J(1,2) = 7.3$ , H–C(1)); 4.56, 4.43 (AB,  $^2J_{AB} = 12.4$ ,  $\text{HOCH}_2 - \text{C}(6)$ ); 4.19 (s, AB,  $^2J_{AB} = 13.0$ ,  $\text{HOCH}_2 - \text{C}(7)$ ); 2.26 (br. s, 2 OH).  $^{13}\text{C-NMR}$  (75 MHz,  $\text{CDCl}_3$ ): 140.56 (C(6)); 140.49 (1 arom. C); 139.62 (1 arom. C); 137.34 (C(12b)); 137.31 (C(4a)); 136.96 (C(7a)); 136.49 (C(8 or 12)); 135.27 (C(5)); 134.85 (C(8 or 12)); 134.12 (C(11)); 132.93 (C(7)); 132.69 (C(12a)); 130.68 (C(10)); 130.47 (2 arom. C); 129.42 (C(2)); 128.95 (C(4)); 128.85 (2 arom. C); 128.77 (C(1)); 127.50 (3 arom. C); 127.03 (C(3)); 126.68 (1 arom. C); 126.20 (2 arom. C); 125.17 (C(9)); 67.12 ( $\text{HOCH}_2 - \text{C}(6)$ ); 59.58 ( $\text{HOCH}_2 - \text{C}(7)$ ). EI-MS: 417 (30,  $[\text{M} + 1]^+$ ), 416 (100,  $\text{M}^+$ ), 399 (21,  $[\text{M} - \text{OH}]^+$ ), 398 (68,  $[\text{M} - \text{H}_2\text{O}]^+$ ), 383 (28,  $[\text{M} - 2\text{OH} + 1]^+$ ), 381 (21,  $[\text{M} - \text{H}_2\text{O} - \text{OH}]^+$ ), 368 (31,  $[\text{M} - \text{CH}_2\text{O} - \text{H}_2\text{O}]^+$ ), 367 (67,  $[\text{M} - \text{CH}_2\text{OH} - \text{H}_2\text{O}]^+$ ), 330 (76,  $[\text{M} - \text{HOCH}_2\text{C}\equiv\text{CCH}_2\text{OH}]^+$ ), 289 (26,  $[\text{M} - \text{HC}\equiv\text{CH} - \text{PhC}\equiv\text{C}]^+$ ), 252 (26,  $[\text{M} - \text{C}_6\text{H}_6 - \text{HOCH}_2\text{C}\equiv\text{CCH}_2\text{OH}]^+$ ), 239 (11,  $[\text{M} - \text{PhC}\equiv\text{C} - \text{C}_6\text{H}_4]^+$ ). Anal. calc. for  $\text{C}_{30}\text{H}_{24}\text{O}_2$  (416.52): C 86.51, H 5.81; found: C 86.80, H 5.54.

1.2.1. *8,12-Diphenylbenzo[a]heptalene-6-methanol-7-[<sup>2</sup>H<sub>2</sub>]methanol* (<sup>2</sup>H<sub>2</sub>-**4b**). Compound **12** (0.022 g, 0.05 mmol) was dissolved in THF (2 ml, dist. over Na) and added dropwise at r.t. to a soln. of LiAlH<sub>4</sub>[<sup>2</sup>H<sub>4</sub>] (2.1 mg, 0.05 mmol) in THF (1 ml, dist. over Na). After stirring for 2 h, a second portion of LiAlH<sub>4</sub>[<sup>2</sup>H<sub>4</sub>] (2.1 mg, 0.05 mmol) was added. The starting material had been consumed after 1 h stirring. The mixture was quenched at 0° by addition of H<sub>2</sub>O (2 drops), followed by KOH (16% in H<sub>2</sub>O; 2 drops) and again H<sub>2</sub>O (6 drops). After vigorous stirring for 30 min, the soln. was dried (Na<sub>2</sub>SO<sub>4</sub>), filtered, and evaporated. CC (silica gel; Et<sub>2</sub>O/hexane 5:1) gave quantitatively <sup>2</sup>H<sub>2</sub>-**4b** as a yellow foam, which crystallized after treatment with Et<sub>2</sub>O/hexane. M.p. 80–100°. R<sub>f</sub> (Et<sub>2</sub>O/hexane 5:1): 0.22. <sup>1</sup>H-NMR (300 MHz, CDCl<sub>3</sub>): Identical with that of **4b** except for *s* at 4.19 (HOCH<sub>2</sub>-C(7)), which was not present. The integration of the residual signal at 4.19 gave 1% <sup>1</sup>H content, *i.e.*, 99% <sup>2</sup>H. The OH signals appeared as br. *s* at 3.0 and 1.6. EI-MS: 419 (12, [M + 1]<sup>+</sup>), 418 (70, M<sup>+</sup>), 400 (63, [M - H<sub>2</sub>O]<sup>+</sup>), 384 (18, [M - 2OH]<sup>+</sup>), 383 (32, [M - H<sub>2</sub>O - OH]<sup>+</sup>), 368 (18, [M - C(<sup>2</sup>H<sub>2</sub>)O - H<sub>2</sub>O]<sup>+</sup>), 367 (62, [M - C(<sup>2</sup>H<sub>2</sub>)OH - H<sub>2</sub>O]<sup>+</sup>), 355 (18, [M - C(<sup>2</sup>H<sub>2</sub>)OH - CH<sub>2</sub>O]<sup>+</sup>), 330 (100, [M - HO(C(<sup>2</sup>H<sub>2</sub>))C≡CCH<sub>2</sub>OH]<sup>+</sup>).

1.3. *2,6,8,10-Tetramethylheptalene-4,5-* (**4c**) and *-heptalene-1,2-dimethanol* (**5c**). The thermal equilibrium mixture of the corresponding dimethyl heptalene-4,5- (**10c**) and heptalene-1,2-dicarboxylates (0.423 g, 1.30 mmol) [15] was dissolved in THF (25 ml) and, after cooling at 0°, reduced with 1M DIBAH soln. in hexane (3.0 ml). Usual workup after 30 min gave a quite unstable oil which was rapidly chromatographed over a short column (silica gel, hexane/Et<sub>2</sub>O). A yellow oil (in total 0.195 g, *ca.* 55%) was obtained, which consisted mainly of a 52:48 mixture **4c/5c**. Since the purified mixture **4c/5c** was still unstable, the two compounds were only characterized by their <sup>1</sup>H-NMR spectra. <sup>1</sup>H-NMR (300 MHz, CDCl<sub>3</sub>) of **4c** (52% in the thermal equilibrium mixture with **5c**): 6.10 (br. *s*, H-C(3,7)); 5.97 (br. *s*, H-C(9)); 5.90 (*q*-like, <sup>4</sup>J(Me-C(2),H-C(1)) = 1.4, H-C(1)); 4.35, 4.31 (*AB*, *J*<sub>AB</sub> = 12.4, <sup>4</sup>J(H-C(3),HOCH<sub>2</sub>-C(4)) = 2.5, HOCH<sub>2</sub>-C(4)); 4.28 (*s*, HOCH<sub>2</sub>-C(5)); residual signals are not assignable). <sup>1</sup>H-NMR (300 MHz, CDCl<sub>3</sub>) of **5c** (48% in the thermal equilibrium mixture): 6.21 (br. *s*, H-C(3)); 5.97 (*quint.*-like, H-C(7 or 9)); 5.90 (br. *s*, H-C(9 or 7)); 5.64 (*d*, <sup>4</sup>J(H-C(3),H-C(5)) = 1.0, H-C(5)); 4.60, 4.04 (*AB*, *J*<sub>AB</sub> = 12.7, HOCH<sub>2</sub>-C(1)); 4.48, 4.19 (*AB*, *J*<sub>AB</sub> = 12.0, HOCH<sub>2</sub>-C(2)); residual signals are not assignable.

1.4. *1,2,6,8,10-Pentmethylheptalene-4,5-dimethanol* (**4d**). Dimethyl heptalene-4,5-dicarboxylate **10d** (0.30 g, 0.88 mmol) [15] was dissolved in THF (20 ml) and reduced with 1M DIBAH soln. in hexane (2 ml) at 0°. The usual workup gave pale yellow crystals of **4d** (0.123, 60%), which were recrystallized from hexane/Et<sub>2</sub>O. M.p. 164–170°. R<sub>f</sub> (Et<sub>2</sub>O): 0.22. <sup>1</sup>H-NMR (300 MHz, CDCl<sub>3</sub>): 6.50 (*s*, H-C(3)); 6.08 (br. *s*, H-C(9)); 5.95 (br. *s*, H-C(7)); 4.38, 4.27 (*AB*, *J*<sub>AB</sub> = 12.6, HOCH<sub>2</sub>-C(4)); 4.30 (*s*, HOCH<sub>2</sub>-C(5)); 2.41 (*q*-like, 2OH); 2.10 (*d*, <sup>4</sup>J(H-C(7),Me-C(6)) ≈ 1.3, Me-C(6)); 1.98 (*d*, <sup>4</sup>J(H-C(9),Me-C(8)) ≈ 1.0, Me-C(8)); 1.91 (br. *s*, Me-C(2)); 1.89 (br. *s*, Me-C(1)); 1.67 (*s*, Me-C(10)). EI-MS: 284 (67, M<sup>+</sup>), 269 (21), 230 (18), 221 (16), 198 (100, [M - HOCH<sub>2</sub>C≡CCH<sub>2</sub>OH]<sup>+</sup>), 183 (22).

1.5. *9-Isopropyl-1,6-dimethylheptalene-4,5-* (**4e**) and *-heptalene-1,2-dimethanol* (**5e**). Dimethyl heptalene-4,5-dicarboxylate **10e** (0.522 g, 1.54 mmol) [23], dissolved in THF (30 ml), was reduced at 0° with 1M DIBAH soln. in hexane. Usual workup and column chromatography (Alox B, act. IV; Et<sub>2</sub>O) gave a thermal equilibrium mixture (0.390 g, 89%) of 82% of **4e** and 18% of **5e** as highly viscous yellow-orange oil. <sup>1</sup>H-NMR (300 MHz, CDCl<sub>3</sub>) of **4e** (82%): 6.44 (*d*, <sup>3</sup>J(2,3) = 6.3, H-C(3)); 6.15 (*d*, <sup>3</sup>J(8,7) = 6.1, H-C(7)); 6.11 (*d*, <sup>3</sup>J(7,8) = 6.1, H-C(8)); 6.05 (*d*, with f.s., <sup>3</sup>J(3,2) = 6.3, H-C(2)); 5.71 (*s*, H-C(10)); 4.37, 4.29 (*AB*, <sup>3</sup>*J*<sub>AB</sub> = 12.7, HOCH<sub>2</sub>-C(4)); 4.33 (*AB*, <sup>3</sup>*J*<sub>AB</sub> ≈ 12, HOCH<sub>2</sub>-C(5)); 2.43 (*sept.*, Me<sub>2</sub>CH); 2.14 (*s*, Me-C(6)); 2.08 (*s*, Me-C(1)); 1.06, 1.02 (*2d*, *J* = 6.9, Me<sub>2</sub>CH); OH signals not recognizable. <sup>1</sup>H-NMR (300 MHz, CDCl<sub>3</sub>) of **5e** (18%): 6.39, 6.38 (*AB*, <sup>3</sup>*J*<sub>AB</sub> ≈ 11.7, H-C(3,4)); 6.37, 6.35 (*AB*, <sup>3</sup>*J*<sub>AB</sub> ≈ 12.6, H-C(8,9)); 5.68 (*s*, H-C(6)); 4.61, 4.10 (*AB*, <sup>2</sup>*J*<sub>AB</sub> = 13.2, HOCH<sub>2</sub>-C(1)); 4.49, 4.24 (*AB*, <sup>2</sup>*J*<sub>AB</sub> = 12.2, HOCH<sub>2</sub>-C(2)); 2.48 (*sept.*, Me<sub>2</sub>CH); 1.73 (*s*, Me-C(5)); 1.67 (*s*, Me-C(10)); 1.13, 1.12 (*2d*, *J* = 7.0, 6.8, Me<sub>2</sub>CH).

**2. Dehydrogenation of the Heptalene-dimethanols with MnO<sub>2</sub>.** - The basic MnO<sub>2</sub> was prepared according to [11]. 2.1. *Dimethanol 4a*. Compound **4a** (0.604 g, 2.23 mmol) was dissolved in CH<sub>2</sub>Cl<sub>2</sub> (115 ml). MnO<sub>2</sub> (11.6 g) was added, and the mixture stirred vigorously during 40 min at r.t. MnO<sub>2</sub> was removed by filtration over *Celite* and washed with CH<sub>2</sub>Cl<sub>2</sub>. To the filtrate was added TsOH (0.06 ml of a 1% soln. in acetone). After 3 h, the soln. was washed with a sat. aq. soln. of NaHCO<sub>3</sub> and dried (MgSO<sub>4</sub>). Column chromatography (silica gel, hexane/Et<sub>2</sub>O 4:1 to 3:2) gave in a first fraction *6,7,9,11-tetramethylheptalenol[1,2-c]furan* (**6a**; 0.350 g, 45%) and, in a second fraction, *1,3-dihydro-6,7,9,11-tetramethylheptalenol[1,2-c]furan-3-one* (**7a**; 0.438 g, 53%).

*Data of 6a*: Light-yellow crystals from hexane at -20°. M.p. 104.8–108.4°. R<sub>f</sub>(hexane/Et<sub>2</sub>O 4:1): 0.57. UV (hexane; *cf.* Fig. 6): λ<sub>max</sub> (see Table 8); λ<sub>min</sub> 315 (3.69), 254 (3.95). IR (CHCl<sub>3</sub>): 3000m, 2962m, 2917m, 2857w, 1626w, 1602m, 1442m, 1374w, 1261s, 1098s, 1012s, 881m, 604w, 588w. <sup>1</sup>H-NMR (300 MHz, CDCl<sub>3</sub>): See Table 5. <sup>1</sup>H-NOE (400 MHz, CDCl<sub>3</sub>): 7.45 (H-C(3))→6.58 (*w*, H-C(4)); 7.12 (H-C(1))→1.85 (*m*, Me-C(11)); 1.85 (Me-C(11))→7.12 (*m*, H-C(1)); 6.12 (*s*, H-C(10)); 1.74 (Me-C(6))→5.95 (*s*, H-C(5)); 1.96 (*m*, Me-C(7)).



$^{13}\text{C}$ -NMR (75 MHz,  $\text{CDCl}_3$ ; assignments via  $^1\text{H}$ ,  $^{13}\text{C}$  correlation spectra at 600 MHz): 139.61 (C(3)); 137.92 (C(1,9)); 136.73 (C(6a)); 134.28 (C(7)); 131.72 (C(5)); 130.54 (C(11a)); 130.19 (C(10)); 127.78 (C(3a,6,8)); 124.98 (C(11b)); 122.01 (C(11)); 120.65 (C(4)); 24.60 (Me–C(9)); 23.09 (Me–C(7)); 20.58 (Me–C(11)); 19.66 (Me–C(6)). EI-MS (see also Table 6): 251 (17,  $[M + 1]^+$ ), 250 (100,  $M^+$ ), 235 (63), 221 (6), 220 (14), 210 (26), 196 (15), 195 (9), 192 (12), 191 (12), 189 (12), 165 (16). Anal. calc. for  $\text{C}_{18}\text{H}_{18}\text{O}$  (250.34): C 86.36, H 7.25; found: C 86.54, H 7.50.

**Data of 7a:** Orange crystals from hexane/ $\text{Et}_2\text{O}$ . M.p. 204–211°.  $R_f$  (hexane/AcOEt 3:2): 0.48. UV (hexane):  $\lambda_{\text{max}}$  ca. 390 (sh with tailing up to 500, 2.84), 371 (3.13), 350 (sh, 3.20), 333 (sh, 3.50), 318 (3.56), 300 (sh, 3.54), 263 (sh, 4.23), 255 (4.35), 248 (sh, 4.23), 206 (4.29);  $\lambda_{\text{min}}$  363 (3.06), 307 (3.52), 228 (4.00). IR ( $\text{CHCl}_3$ ): 3006w, 2947w, 2918w, 1756s, 1628w, 1601w, 1445m, 1376w, 1333m, 1280w, 1147w, 1092m, 1032s.  $^1\text{H}$ -NMR (300 MHz,  $\text{CDCl}_3$ ): 6.61 (dd,  $^3J(5,4) = 11.5$ ,  $^5J(\text{H}_A\text{--C}(1),4) \approx 1$ , H–C(4)); 6.56 (d,  $^3J(4,5) = 11.5$ , H–C(5)); 6.09 (br. s, H–C(10)); 6.00 (quint.-like br. s, H–C(8)); 5.11 (dd, A of AB,  $^2J_{AB} = 17.7$ ,  $^3J(4, \text{H}_A) \approx 1$ ,  $\text{H}_A\text{--C}(1)$ ); 4.55 (d, B of AB,  $^2J_{AB} = 17.8$ ,  $\text{H}_B\text{--C}(1)$ ); 2.00 (d,  $^4J(10, \text{Me--C}(9)) = 1.2$ , Me–C(9)) = 1.2, Me–C(9)); 1.96 (d,  $^4J(8, \text{Me--C}(7)) = 1.3$ , Me–C(7)); 1.76 (s, Me–C(11)); 1.75 (s, Me–C(6)).  $^1\text{H}$ -NOE (400 MHz,  $\text{CDCl}_3$ ): 1.76/1.77 (Me–C(6,11)) → 6.56 (s, H–C(5)); 6.09 (s, H–C(10)); 5.11 (s,  $\text{H}_A\text{--C}(1)$ ); and 1.96 (s, Me–C(7)). The  $^1\text{H}$ -NOE shows that  $\text{H}_A\text{--C}(1)$  represents  $\text{H}_{RS}\text{--C}(1)$  and  $\text{H}_B\text{--C}(1)$  correspondingly  $\text{H}_{SR}\text{--C}(1)$  in (PM)-7a (cf. Scheme 10 and Table 3). EI-MS: 267.2 (16,  $[M + 1]^+$ ), 266.2 (100,  $M^+$ ), 264.1 (18,  $[M - 2 \text{H}]^+$ ), 251.1 (35,  $[M - \text{Me}]^+$ ), 226.2 (87,  $[M - \text{MeC}\equiv\text{CH}]^+$ ), 212.1 (89,  $[M - 54]^+$ ). Anal. calc. for  $\text{C}_{18}\text{H}_{18}\text{O}_2$  (266.34): C 81.17, H 6.81; found: C 81.25, H 6.57.

**2.2. Dimethanol (–)-(P)-5a.** The compound (0.0586 g, 0.217 mmol) was reacted with  $\text{MnO}_2$  as described under 2.1. Prep. TLC (silica gel; hexane/ $\text{Et}_2\text{O}$  7:3) gave (–)-(P)-6a (0.019 g, 35%), (–)-(P)-7a (0.0115 g, 20%), and a 81:19 mixture (0.0069 g, 10 and 2%, resp.) of 8a and the dicarbaldehyde 9a.

**Data of (–)-(P)-6a:** Light-yellow crystals from hexane at  $-20^\circ$ . M.p. 116.1–118.1°. CD (hexane; cf. Table 7): 320.6 (–26.9), 297 (sh, –20.5), 275.0 (0), 258 (sh, 15.1), 232.8 (sh, 76.6); 223.2 (93.0), 207.4 (0). The racemization was followed in heptane ( $c = 4.57 \cdot 10^{-5}$  M) at  $120.0^\circ$  by measuring the decrease of  $\Delta\epsilon$  of the band at 223 nm during 1.4 half-live times;  $k_{\text{rac}} = 6.50 \cdot 10^{-5} \text{ s}^{-1}$  ( $r = 0.9987$ ).

**Data of (–)-(P)-7a:** Orange crystals from hexane/ $\text{Et}_2\text{O}$ . M.p. 185.0–186.2°. CD (hexane; cf. Fig. 2): 392.4 (–6.3), 357.0 (–4.66), 315.0 (–17.8), 292.0 (0), 269.4 (70.5), 249.0 (0), 246.2 (–1.8), 242.8 (0), 220.4 (35.2), 207.3 (0).

**1,3-Dihydro-6,7,9,11-tetramethylheptaleno[1,2-c]furan-1-one (8a):** In the mixture with 19% of 9a.  $^1\text{H}$ -NMR: 6.71 (d,  $J(5,4) = 11.4$ , H–C(4)); 6.35 (d,  $J(4,5) = 11.4$ , H–C(5)); 6.12 (br. s, H–C(10)); 6.00 (br. s, quint.-like, H–C(8)); 4.94, 4.82 (AB,  $J_{AB} = 16.7$ ,  $\text{H}_2\text{C}(3)$ );  $\text{H}_A$  (4.94) shows a further coupling (0.6 Hz), presumably with H–C(5)); 1.99 (d,  $J(10, \text{Me--C}(9)) = 1.3$ , Me–C(9)); 1.96 (d,  $J(9, \text{Me--C}(7)) = 1.4$ , Me–C(7)); 1.77 (s, Me–C(6)); 1.68 (s, Me–C(11)).

**1,6,8,10-Tetramethylheptalene-4,5-dicarbaldehyde (9a):** In the mixture with 81% of 8a.  $^1\text{H}$ -NMR: 9.92 (s, HC(O)–C(4)); height of s  $\frac{1}{2}$  of that at 9.49; 9.49 (s, HC(O)–C(5)); 7.29 (d, quint.-like,  $J(2,3) = 5.7$ ,  $^4J(\text{HC(O)–C}(4),3) \approx ^5J(\text{Me--C}(1),3) \approx 0.7$ , H–C(3)); 6.40 (dq,  $J(3,2) = 5.7$ ,  $J(\text{Me--C}(1),2) = 1.4$ , H–C(2)); 6.20 (br. s, H–C(9)); 6.17 (br. s, quint.-like, H–C(7)); 2.15 (d,  $J(7, \text{Me--C}(6)) = 1.4$ , Me–C(6)); 2.06 (d,  $J(9, \text{Me--C}(8)) = 1.2$ , Me–C(8)); 2.05 (t-like,  $^4J(2, \text{Me--C}(1)) \approx ^5J(3, \text{Me--C}(1)) \approx 1.2$ , Me–C(1)); 1.79 (s, Me–C(10)).

**2.3. Dimethanol 4b.** The compound (0.059 g, 0.142 mmol) was reacted with  $\text{MnO}_2$  in analogy to 2.1 during 2 h. Workup gave crystalline 1,3-dihydro-9,13-diphenylbenzo[1,2]heptaleno[4,5-c]furan-3-one (11b). It formed orange-red crystals (0.040 g, 68%) after recrystallization from  $\text{Et}_2\text{O}$ /hexane and melted at 180–182°, recrystallized and melted again at 223–227°.  $R_f$  (hexane/ $\text{Et}_2\text{O}$  4:1): 0.25. UV (hexane):  $\lambda_{\text{max}}$  374 (3.65; long tailing up to 520), 317 (sh, 4.14), 278 (4.40), 234 (4.42), 220 (4.44);  $\lambda_{\text{min}}$  349 (3.59), 255 (4.38), 230 (4.42), 218 (4.44). IR (KBr): 3040w, 3019w, 1762s, 1637w, 1613w, 1597w, 1552w, 1488w, 1444w, 1345m, 1258w, 1236w, 1171s, 1148m, 1075w, 1060m, 1010s, 949w, 899w, 796w, 755s, 699s, 623w, 610w, 574w.  $^1\text{H}$ -NMR (300 MHz,  $\text{CDCl}_3$ ): 7.94 (s, H–C(4)); 7.51 (d, with f.s., H–C(5)); 7.3–7.2 (m, 7 H); 7.04 (m, 3 H); 6.91 (d,  $^3J(11,12) = 6.0$ , H–C(12)); 7.75 (m, 3 H); 6.61 (m, 2 H); 4.47, 3.93 (AB,  $^2J_{AB} = 13.2$ ,  $\text{CH}_2(1)$ ). EI-MS: 413 (22,  $[M + 1]^+$ ), 412 (100,  $M^+$ ), 382 (16,  $[M - \text{CH}_2\text{O}]^+$ ), 356 (8), 355 (10), 354 (7), 352 (9), 351 (8), 350 (7), 310 (18). Anal. calc. for  $\text{C}_{30}\text{H}_{20}\text{O}_2$  (412.49): C 87.36, H 4.89; found: C 87.18, H 4.81.

**2.3.1. Dimethanol  $f^2\text{H}_2$ -4b.** The compound (0.0171 g, 0.04 mmol) was dissolved in  $\text{CH}_2\text{Cl}_2$  (2 ml; dist. over  $\text{CaH}_2$ ) and  $\text{MnO}_2$  (0.325 g) added. Stirring for 2 h at r.t. and workup gave  $[1\text{-}^2\text{H}_2]\text{-11b}$  (0.0096 g, 58%) as orange woolly crystals. M.p. 184.8–186.8°, followed by recrystallization and again melting at 193.5–195.2°.  $^1\text{H}$ -NMR: identical with that of 11b. However, no signals were present at 4.47 and 3.93 (AB of  $\text{CH}_2(1)$ ). EI-MS: 415 (30,  $[M + 1]^+$ ), 414 (100,  $M^+$ ), 382 (5,  $[M - \text{C}^2\text{H}_2\text{O}]^+$ ), 353 (8,  $[M - \text{HC}^2\text{H}_2\text{O}]^+$ ), 312 (45,  $[M - \text{PhC}\equiv\text{CH}]^+$ ), 254 (10,  $[M - \text{C}^2\text{H}_2]\text{C}\equiv\text{CCO} - \text{C}_6\text{H}_4]^+$ ), 253 (10,  $[M - \text{C}^2\text{H}_2]\text{C}\equiv\text{CCO} - \text{Ph}]^+$ ), 236 (21,  $[M - \text{PhC}\equiv\text{CH} - \text{C}_6\text{H}_4]^+$ ).

2.4. *Dimethanols 4c and 5c.* Dimethyl heptalene-dicarboxylates **10c** and its DBS isomer (0.382 g, 1.17 mmol) were reduced with DIBAH (see 1.3) and the crude dimethanol mixture dissolved in  $\text{CH}_2\text{Cl}_2$  (100 ml). Dehydrogenation with  $\text{MnO}_2$  was performed according to 2.1. The chromatographic workup (silica gel, hexane/ $\text{Et}_2\text{O}$  3:2) gave in a first fraction (0.067 g, 23%) 5,7,9,11-tetramethylheptaleno[1,2-c]furan (**6c**), followed by a second fraction (0.048 g, 16%) of 1,3-dihydro-5,7,9,11-tetramethylheptaleno[1,2-c]furan-3-one (**7c**) and, finally, by a third fraction (0.027 g, 9%) of 1,3-dihydro-5,7,9,11-tetramethylheptaleno[1,2-c]furan-1-one (**8c**).

*Data of 6c:* Yellow crystals from hexane. M.p. 177.5–178.9°.  $R_f$  (hexane/ $\text{Et}_2\text{O}$  7:3): 0.48. UV (hexane; cf. Fig. 7);  $\lambda_{\text{max}}$  (see Table 8);  $\lambda_{\text{min}}$  317 (3.71), 257 (3.95). IR ( $\text{CHCl}_3$ ): 3003s, 2974m, 2942m, 2916s, 2872w, 2857w, 1649w, 1634w, 1595w, 1520w, 1438s, 1376m, 1261m, 1128m, 1097w, 1051s, 1016s, 890w, 864s, 602m, 591m.  $^1\text{H-NMR}$  (300 MHz,  $\text{CDCl}_3$ ): see Table 5.  $^1\text{H-DR}$  (400 MHz,  $\text{CDCl}_3$ ): 6.37 (H-C(4))→7.11 (d,  $^5J(1,3) = 1.5$ , H-C(3)) and 1.92 (s, Me-C(5)).  $^1\text{H-NOE}$  (400 MHz,  $\text{CDCl}_3$ ): 5.53 (H-C(6))→2.08 (s, Me-C(7)) and 1.92 (s, Me-C(5)); 1.87 (Me-C(11))→7.11 (m, H-C(1)) and 6.08 (s, H-C(10)). EI-MS (see also Table 6): 251 (17,  $[M + 1]^+$ ), 250 (100,  $M^+$ ), 235 (26), 221 (5), 220 (5), 210 (49), 196 (11), 195 (12), 165 (14). Anal. calc. for  $\text{C}_{18}\text{H}_{18}\text{O}$  (250.34): C 86.36, H 7.25; found: C 86.65, H 7.25.

*Data of 7c:* Orange crystals from hexane/toluene. M.p. 219–222°.  $R_f$  (hexane/ $\text{Et}_2\text{O}$  7:3): 0.21. UV (hexane):  $\lambda_{\text{max}}$  390 (sh, 2.89; tailing up to 510), 327 (3.71), 261 (4.34), 249 (sh, 4.29), 204 (4.34);  $\lambda_{\text{min}}$  299 (3.53), 228 (4.05), 195 (4.32). IR ( $\text{CHCl}_3$ ): 3030w, 3006w, 2978w, 2945w, 2918w, 1757s, 1616w, 1443w, 1397w, 1377w, 1344w, 1317w, 1167w, 1119w, 1033m, 894w, 877w, 858w, 842w.  $^1\text{H-NMR}$  (400 MHz,  $\text{CDCl}_3$ ): 6.35 (q-like,  $^4J(\text{Me-C}(5),4) \approx 0.9$ , H-C(4)); 6.05 (br. s, H-C(10)); 5.88 (quint.-like s, H-C(8)); 5.53 (s, H-C(6)); 5.08 and 4.54 (AB,  $^2J_{AB} = 17.6$ ,  $\text{CH}_2(1)$ ); 2.05 (d,  $^4J(8,\text{Me-C}(7)) = 1.2$ , Me-C(7)); 2.02 (br. s, Me-C(5)); 1.95 (d,  $^4J(10,\text{Me-C}(9)) = 1.2$ , Me-C(9)); 1.73 (s, Me-C(11)).  $^1\text{H-NOE}$  (400 MHz,  $\text{CDCl}_3$ ): 6.35 (H-C(4))→2.02 (s, Me-C(5)); 5.53 (H-C(6))→2.05 (s, Me-C(7)) and 2.02 (s, Me-C(5)); 1.73 (Me-C(11))→6.05 (s, H-C(10)) and 5.08 (s, H-C(1)). The  $^1\text{H-NOE}$  shows that  $\text{H}_A\text{-C}(1)$  represents  $\text{H}_{SR}\text{-C}(1)$  and  $\text{H}_B\text{-C}(1)$  correspondingly  $\text{H}_{SR}\text{-C}(1)$  in (PM)-**7c**. EI-MS: 267.2 (11,  $[M + 1]^+$ ), 266.2 (64,  $M^+$ ), 251.2 (5,  $[(M + 1) - \text{Me}]^+$ ), 227.2 (15,  $[(M + 1) - \text{MeC}\equiv\text{CH}]^+$ ), 226.2 (100,  $[M - \text{MeC}\equiv\text{CH}]^+$ ). Anal. calc. for  $\text{C}_{18}\text{H}_{18}\text{O}_2$  (266.34): C 81.17, H 6.81; found: C 81.38, H 6.64.

*Data of 8c:* Red crystals from hexane/toluene. M.p. 200.2–201.5°.  $R_f$  (hexane/ $\text{Et}_2\text{O}$  3:2): 0.13. UV (hexane):  $\lambda_{\text{max}}$  420 (sh, 2.85), 322 (sh, 3.66), 307 (sh, 3.70), 268 (4.37), 246 (sh, 4.23), 205 (4.40);  $\lambda_{\text{min}}$  228 (4.13). IR ( $\text{CHCl}_3$ ): 3007w, 2918w, 1744s, 1608m, 1448m, 1320m, 1125w, 1041w.  $^1\text{H-NMR}$ : 6.11 (br. s, H-C(10)); 6.07 (br. s, H-C(4)); 5.89 (br. s, quint.-like, H-C(8)); 5.54 (d,  $J(4,6) \approx 0.8$ , H-C(6)); 4.84, 4.72 (AB,  $J_{AB} = 17.0$ ,  $\text{CH}_2(3)$ ); 2.06 (d,  $J(8,\text{Me-C}(7)) = 1.2$ , Me-C(7)); 2.05 (d,  $J(4,\text{Me-C}(5)) = 1.2$ , Me-C(5)); 1.93 (d,  $J(10,\text{Me-C}(9)) = 1.3$ , Me-C(9)); 1.65 (s, Me-C(11)).  $^1\text{H-NOE}$  (400 MHz,  $\text{CDCl}_3$ ): 6.11 (H-C(10))→1.93 (s, Me-C(9)); 1.65 (s, Me-C(11)); 6.07 (H-C(4))→2.05 (s, Me-C(5)); 5.54 (H-C(6))→2.06 (s, Me-C(7)); 2.05 (s, Me-C(5)); 1.65 (Me-C(11))→6.11 (s, H-C(10)). EI-MS: 267 (18,  $[M + 1]^+$ ), 266 (100,  $M^+$ ), 251 (9,  $[M - \text{Me}]^+$ ), 227 (11), 226 (73), 212 (17), 207 (10), 179 (10), 178 (9), 165 (19), 152 (9). Anal. calc. for  $\text{C}_{18}\text{H}_{18}\text{O}_2$  (266.34): C 81.17, H 6.81; found: C 81.34, H 6.62.

2.5. *Dimethanol 4d.* The oxidation of the diol (0.072 g; 0.253 mmol) with  $\text{MnO}_2$  in the usual manner gave, after separation by prep. TLC (hexane/ $\text{Et}_2\text{O}$  4:1), 5,6,7,9,11-pentamethylheptaleno[1,2-c]furan (**6d**) (0.0222 g, 33%) and 1,3-dihydro-5,6,7,9,11-pentamethylheptaleno[1,2-c]furan-3-one (**7d**) (0.0327 g, 46%).

*Data of 6d:* Light-yellow crystals from hexane. M.p. 163.2–164.1°.  $R_f$  (hexane/ $\text{Et}_2\text{O}$  3:2): 0.58. UV (hexane; cf. Fig. 8);  $\lambda_{\text{max}}$  (see Table 8);  $\lambda_{\text{min}}$  253 (4.05). IR ( $\text{CHCl}_3$ ): 3000s, 2974s, 2915s, 2858m, 1628w, 1601w, 1445s, 1374m, 1262m, 1102m, 1044s, 887s, 847s, 590m.  $^1\text{H-NMR}$  (400 MHz,  $\text{CDCl}_3$ ): see Table 5.  $^1\text{H-NOE}$  (400 MHz,  $\text{CDCl}_3$ ): 2.008 (Me-C(9))→6.114 (s, H-C(10)); 5.995 (s, H-C(8)); 1.975 (Me-C(5))→6.495 (s, H-C(4)); 1.751 (m, Me-C(6)); 1.854 (Me-C(11))→7.091 (s, H-C(1)); 6.114 (s, H-C(10)). EI-MS (see also Table 6): 265 (15,  $[M + 1]^+$ ), 264 (91,  $M^+$ ), 249 (100), 235 (8), 234 (23), 235 (8), 224 (6), 221 (10), 210 (77), 189 (15), 181 (14), 165 (21). Anal. calc. for  $\text{C}_{19}\text{H}_{20}\text{O}$  (264.37): C 86.32, H 7.63; found: C 86.30, H 7.46.

*Data of 7d:* Orange crystals from hexane/toluene. M.p. 208.3–210.1°.  $R_f$  (hexane/ $\text{Et}_2\text{O}$  3:2): 0.30. UV (hexane):  $\lambda_{\text{max}}$  374 (sh, 3.10), 312 (sh, 3.60), 264 (4.34);  $\lambda_{\text{min}}$  230 (4.10). IR ( $\text{CDCl}_3$ ): 3006m, 2973m, 2916m, 1751s, 1632w, 1445m, 1376w, 1347w, 1324m, 1286w, 1262w, 1109m, 1029s, 1001m, 847w.  $^1\text{H-NMR}$  (400 MHz,  $\text{CDCl}_3$ ): 6.497 (br. s, H-C(4)); 6.067 (br. s, H-C(10)); 5.977 (br. s, quint.-like, H-C(8)); 5.092, 4.538 (AB,  $^2J_{AB} = 17.6$ ,  $\text{H}_2\text{C}(1)$ ); 2.077 (br. s, Me-C(5)); 2.008 (d,  $^4J(10,\text{Me-C}(9)) = 1.2$ , Me-C(9)); 1.951 (d,  $^4J(8,\text{Me-C}(7)) = 1.3$ , Me-C(7)); 1.761 (s, Me-C(11)); 1.743 (s, Me-C(6)).  $^1\text{H-NOE}$  (400 MHz,  $\text{CDCl}_3$ ): 2.077 (Me-C(5))→6.497 (s, H-C(4)); 1.743 (s, Me-C(6)); 2.008 (Me-C(9))→6.067 (s, H-C(10)); 5.977 (s, H-C(8)). EI-MS: 281 (15,  $[M + 1]^+$ ), 280 (93,  $M^+$ ), 265 (36), 240 (58), 226 (100), 221 (16), 197 (30), 178 (11), 165 (11). Anal. calc. for  $\text{C}_{19}\text{H}_{20}\text{O}_2$  (280.37): C 81.40, H 7.19; found: C 81.31, H 6.89.

2.6. *Dimethanols 4e and 5e.* The equilibrium mixture **4e/5e** (0.310 g, 1.09 mmol) was reacted with  $\text{MnO}_2$  in the usual manner (see 2.1) during 75 min. CC on silica gel (hexane/ $\text{Et}_2\text{O}$  1:1) gave in the indicated order 8-isopropyl-

6,11-dimethylheptalenol[1,2-c]furan (**6e**) (0.0831 g, 29%) and 1,3-dihydro-8-isopropyl-6,11-dimethylheptalenol[1,2-c]furan-3-one (**7a**) (0.1118 g, 37%). In a second run, where the mixture **4e/5e** was not further purified, but just reacted with  $\text{MnO}_2$ , we found beside **6e** and **7e** in the last fractions of the chromatography ca. 5% of 1,3-dihydro-8-isopropyl-6,11-dimethylheptalenol[1,2-c]furan-1-one (**8e**). To ascertain that **8e** was a product of the  $\text{MnO}_2$  reaction of **4e/5e** and not already formed in the reduction of **10e**, the crude mixture **4e/5e** from the reduction of **10e** was carefully analyzed by  $^1\text{H-NMR}$ . The signals of the *AB* system of  $\text{H}_2\text{C}(3)$  of **8e** could not be found within the limits of detection ( $\geq 0.5\%$ ).  $\text{MnO}_2$  Reaction of this mixture and, again, analysis of the crude oxidized mixture by  $^1\text{H-NMR}$  showed the presence of 50% of **6e**, 46% of **7e** and its DBS isomer **11e** (see below), and 4% of **8e**.

*Data of 6e*: Yellow oil.  $R_f$  (hexane/ $\text{Et}_2\text{O}$  9:1): 0.50. UV (hexane):  $\lambda_{\text{max}}$  (see *Table 8*);  $\lambda_{\text{min}}$  320 (4.02), 257 (4.26). IR ( $\text{CHCl}_3$ ): 3005s, 2962s, 2869m, 1626m, 1598w, 1567w, 1542w, 1464m, 1375m, 1262w, 1132w, 1049s, 1007m, 887s, 597s.  $^1\text{H-NMR}$  (300 MHz,  $\text{CDCl}_3$ ): see *Table 5*.  $^1\text{H-NOE}$  (400 MHz,  $\text{CDCl}_3$ ): 1.886 (Me-C(11))  $\rightarrow$  7.163 (s, H-C(1)); 6.353 (s, H-C(10)); 1.738 (Me-C(6))  $\rightarrow$  5.956 (s, H-C(5)); 5.694 (s, H-C(7)). EI-MS (see also *Table 6*): 265 (27,  $[M + 1]^+$ ), 264 (100,  $M^+$ ), 249 (19), 235 (2), 234 (4), 224 (15), 221 (17), 209 (14), 196 (18), 189 (9), 178 (9), 165 (13).

*Data of 7e*: Red crystals from hexane/AcOEt. M.p. 113.3–114.2°.  $R_f$  (hexane/ $\text{Et}_2\text{O}$  3:2): 0.30. UV (hexane, cf.  $^1\text{H-NMR}$ ):  $\lambda_{\text{max}}$  400 (very br. sh, 2.78), 314 (sh, 3.56), 262 (4.37), 201 (4.33);  $\lambda_{\text{min}}$  229 (4.04). IR (KBr): 3014w, 2960m, 1733s, 1442m, 1365w, 1332m, 1287m, 1183w, 1026s, 988w, 780m, 754m.  $^1\text{H-NMR}$  (300 MHz,  $\text{CDCl}_3$ ; in the presence of 22% of its DBS isomer **11e**): 6.537, 6.536 (*AB*,  $^3J_A \approx 11.3$ , H-C(4 and 5)); 6.397 (*d*,  $^3J(10,9) = 11.9$ , H-C(9)); 6.324 (*d*,  $^3J(9,10) = 11.9$ , H-C(10)); 5.507 (br. s, H-C(7)); 5.116, 4.591 (*AB*,  $^2J_{AB} = 17.8$ ,  $\text{CH}_2(1)$ ); 2.510 (*sept.*,  $\text{Me}_2\text{CH}$ ); 1.763 (s, Me-C(11)); 1.706 (s, Me-C(6)); 1.133, 1.112 (*2d*,  $J = 6.6$ ,  $\text{Me}_2\text{CH}$ ).  $^1\text{H-NOE}$  (400 MHz,  $\text{CDCl}_3$ ): 1.763 (Me-C(11))  $\rightarrow$  6.324 (s, H-C(10)); 5.116 (s,  $\text{H}_{RS}\text{-C}(1)$ ; cf. *Scheme 10*); 1.706 (Me-C(6))  $\rightarrow$  6.536 (s, H-C(5)); 5.507 (s, H-C(7)). EI-MS: 281 (18,  $[M + 1]^+$ ), 280 (100,  $M^+$ ), 265 (17), 240 (58), 225 (32), 212 (100), 183 (14), 178 (11), 165 (18), 152 (11). Anal. calc. for  $\text{C}_{19}\text{H}_{20}\text{O}_2$  (280.77): 81.36, H 7.19; found: C 81.38, H 6.91.

1,3-Dihydro-8-isopropyl-6,11-dimethylheptalenol[4,5-c]furan-3-one (**11e**): In thermal equilibrium with 78% of **7e**.  $^1\text{H-NMR}$  (300 MHz,  $\text{CDCl}_3$ ): 7.066 J(*d*,  $^3J(5,4) = 6.7$ , H-C(4)); 6.262 (*dq*-like,  $^3J(4,5) = 6.7$ , H-C(5)); 6.171 (*dq*-like,  $^3J(9,10) = 6.5$ , H-C(10)); 6.015 (br. *d*,  $^3J(10,9) \approx 6.8$ , H-C(9)); 5.638 (s, H-C(7)); 4.763, 4.514 (*AB*,  $^2J_{AB} = 12.8$ ,  $\text{CH}_2(1)$ ); 2.049 (*sept.*,  $\text{Me}_2\text{CH}$ ); 2.226 (*dd*,  $^4J_5\text{Me-C}(6) = 1.3$ ,  $^5J(4,\text{Me-C}(6)) = 0.7$ , Me-C(6)); 1.967 (br. s, Me-C(11)); 1.070, 1.041 (*2d*,  $J = 6.8$ ,  $\text{Me}_2\text{CH}$ ).  $^1\text{H-NOE}$  (400 MHz,  $\text{CDCl}_3$ ): 2.226 (Me-C(6))  $\rightarrow$  6.262 (s, H-C(5)); 5.638 (s, C(7)); 1.967 (Me-C(11))  $\rightarrow$  6.171 (s, H-C(10)); 4.763 (s,  $\text{H}_{RS}\text{-C}(1)$ ; cf. *Scheme 10*).

1,3-Dihydro-8-isopropyl-6,11-dimethylheptalenol[1,2-c]furan-1-one (**8e**): Red oil, ca. 95%.  $R_f$  (hexane/ $\text{Et}_2\text{O}$  3:2): 0.18.  $^1\text{H-NMR}$  (300 MHz,  $\text{CDCl}_3$ ): 6.657 (*d*,  $^3J(5,4) = 11.3$ , H-C(4)); 6.361 (*d*,  $^3J(9,10) = 11.8$ , H-C(10)); 6.341 (*dd*-like  $^3J(10,9) = 11.8$ ,  $^4J(7,9) = 1.2$ , H-C(9)); 6.261 (*d*,  $^3J(4,5) = 11.3$ , H-C(5)); 5.485 (s, H-C(7)); 4.878, 4.752 (*AB*,  $^2J_{AB} = 16.8$ ,  $\text{CH}_2(3)$ ); 2.497 (*sept.*,  $\text{Me}_2\text{CH}$ ); 17.20 (s, Me-C(6)); 1.673 (s, Me-C(11)); 1.130, 1.107 (*2d*, superimp. to *t*,  $J = 6.8$ ,  $\text{Me}_2\text{CH}$ ).

**3. Methylenation of Heptalenol[1,2-c]furan-3-ones **7** with *Tebbe's* Reagent.** – 3.1 *Formation of 3,6,7,9,11-Pentamethylheptalenol[1,2-c]furan (23a)*. Furanone **7a** (0.1625 g, 0.611 mmol) was dissolved in dry THF (10 ml). At  $-25$  to  $-30^\circ$ , the *Tebbe's* reagent (*Aldrich*®; 1.4 ml of a 0.5M soln. in toluene) was added dropwise under stirring. Stirring was continued for 15 min at  $-25$  to  $-30^\circ$ . The mixture was then added to a mixture of  $\text{Et}_2\text{O}$  (10 ml) and 0.5N aq. NaOH (0.25 ml) and stirred for an additional h at r.t. The org. layer was dried ( $\text{MgSO}_4$ ) and filtered over *Celite*. The org. solvents were evaporated and the residue subjected to CC (silica gel; hexane/ $\text{Et}_2\text{O}$  4:1). Compound **23a** (0.1015 g, 63%) was obtained as a yellow oil.  $R_f$  (hexane/ $\text{Et}_2\text{O}$  7:3): 0.58 UV (hexane; see also *Fig. 9*):  $\lambda_{\text{max}}$  (see *Table 8*);  $\lambda_{\text{min}}$  256.8 (3.92). IR ( $\text{CHCl}_3$ ): 3001s, 2942s, 2935s, 2917s, 2858m, 1631s, 1561m, 1443s, 1391m, 1375m, 1268w, 1122m, 1027w, 1000w, 932m, 902m, 846m.  $^1\text{H-NMR}$  (300 MHz,  $\text{CDCl}_3$ ): see *Table 5*.  $^1\text{H-NOE}$  (400 MHz,  $\text{CDCl}_3$ ): 2.327 (Me-C(3))  $\rightarrow$  6.485 (s, H-C(4)); 1.866 (Me-C(11))  $\rightarrow$  6.987 (m, H-C(1)), 6.119 (s, H-C(10)). EI-MS (see also *Table 6*): 265 (22,  $[M + 1]^+$ ), 264 (100,  $M^+$ ), 249 (41), 235 (5), 234 (11), 224 (21), 221 (4), 210 (13), 191 (6), 189 (7), 165 (10), 85 (11), 83 (17), 43 (6).

3.2. *Formation of 8-Isopropyl-3,6,11-trimethylheptalenol[1,2-c]furan (23e)*. Furanone **7e** (0.104 g, 0.371 mmol) was dissolved in dry THF (8 ml) and reacted with *Tebbe* reagent (0.8 ml of a 0.5M soln. in toluene) as described under 3.1. Purification of the residue of the mixture by prep. TLC (silica gel; hexane/ $\text{Et}_2\text{O}$  7:3) gave pure **23e** (0.0465 g, 45%), which was recrystallized from hexane. M.p. 108–109°.  $R_f$  (hexane/ $\text{Et}_2\text{O}$  3:2): 0.60 UV (hexane):  $\lambda_{\text{max}}$  (see *Table 8*);  $\lambda_{\text{min}}$  260 (3.87). IR ( $\text{CHCl}_3$ ): 3005s, 2962s, 2920s, 2870m, 1632m, 1600w, 1558m, 1464m, 1376m, 1293w, 1271w, 1121m, 1063w, 1033w, 998w, 923w, 896w.  $^1\text{H-NMR}$  (300 MHz,  $\text{CDCl}_3$ ): see *Table 5*. EI-MS (see also *Table 6*): 279 (22,  $[M + 1]^+$ ), 278 (100), 263 (13), 249 (1), 248 (3), 238 (6), 235 (8), 223 (8), 210 (8), 189 (3), 178 (2), 165 (4). Anal. calc. for  $\text{C}_{20}\text{H}_{22}\text{O}$  (278.40): C 86.29, H 7.97; found: C 86.47, H 7.68.

**4. Chromatographic Separation of the Heptaleno[1,2-*c*]furans into Their Antipodes.** – The HPLC separations were performed on an analytical *Chiralcel OD* column (4.6 × 300 mm) from *Daicel* with hexane as eluant. Whereas **6a** and **6e** could not be separated under these conditions, the heptaleno[1,2-*c*]furans **6a**, **6d**, and **23a** showed base-line separations of their antipodes with the following  $t_R$  values at a flow-rate of 0.5 ml/min: (–)-(P)-**6a**: 15.2 min, (+)-(M)-**6a**: 21.7 min; (–)-(P)-**6d**: 13.6 min; (+)-(M)-**6d**: 19.1 min; (–)-(P)-**23a**: 13.0 min, (+)-(M)-**23a**: 38.8 min.

CD (hexane) of (–)-(P)-**6a** (see Fig. 3 and Table 7): 275 (0), 207 (0). CD (hexane) of (+)-(M)-**6a** (see Fig. 3): 319 (25.3), 297 (sh, 19.9), 275 (0), 257 (sh, –14.3), 233 (sh, –71.3), 223 (–87.3), 208 (0).

CD (hexane) of (+)-(M)-**6d** (see Fig. 4): 314 (29.7), 272 (0), 260 (sh, –9.3), 235 (–89.0), 230 (sh, –86.4), 207 (0).

The racemization of (+)-(M)-**6d** was followed in heptane ( $c = 4.67 \cdot 10^{-5}$  M) at 120.0° by measuring the decrease of  $\Delta\epsilon$  of the band at 235 nm during 1.5 half-life times;  $k_{\text{rac}} = 5.58 \cdot 10^{-5} \text{ s}^{-1}$  ( $r = 0.9994$ ).

CD (hexane) of (–)-(P)-**23a** (see Fig. 5 and Table 7): 280 (0). CD (hexane) of (+)-(M)-**23a** (see Fig. 5): 319 (32.5), 280 (0), 257 (sh, –17.4), 237 (–76.0), 228 (sh, –73.1).

#### REFERENCES

- [1] A Guide to IUPAC Nomenclature of Organic Compounds, Recommendations 1993, prepared for publ. by R. Panico, W. H. Powell, J.-C. Richer, Blackwell Scientific Publ., Oxford 1993.
- [2] R.-A. Fallahpour, H.-J. Hansen, *Helv. Chim. Acta* **1995**, *78*, 0000.
- [3] W. Bernhard, P. Brügger, J. J. Daly, P. Schönholzer, R. H. Weber, H.-J. Hansen, *Helv. Chim. Acta* **1985**, *68*, 415.
- [4] R. H. Weber, P. Brügger, T. A. Jenny, H.-J. Hansen, *Helv. Chim. Acta* **1987**, *70*, 742.
- [5] R. H. Weber, P. Brügger, W. Arnold, P. Schönholzer, H.-J. Hansen, *Helv. Chim. Acta* **1987**, *70*, 1439.
- [6] P. A. Stadler, *Helv. Chim. Acta* **1978**, *61*, 1675.
- [7] A. J. Fatiadi, *Synthesis* **1976**, 65 and 133; A. J. Fatiadi, in 'Organic Synthesis by Oxidation with Metal Compounds', Eds. W. J. Mijs, C. R. H. I. de Jonge, Plenum Press, New York–London, 1986, p. 119 ff.
- [8] S. Hauptmann, A. Blaskovits, *Z. Chem.* **1966**, *6*, 466.
- [9] R.-A. Fallahpour, R. Sigrüst, H.-J. Hansen, *Helv. Chim. Acta* **1995**, *78*, 1408.
- [10] a) W. Bernhard, P. Brügger, P. Schönholzer, R. H. Weber, H.-J. Hansen, *Helv. Chim. Acta* **1985**, *68*, 429; b) K. Hafner, G. L. Knaup, H. J. Lindner, H.-C. Flöter, *Angew. Chem.* **1985**, *97*, 209; *ibid. Int. Ed.* **1985**, *24*, 212; K. Hafner, G. L. Knaup, *Tetrahedron Lett.* **1986**, *27*, 1665.
- [11] 'Vogel's Textbook of Practical Organic Chemistry', 4th edn., Longman Scientific & Technical, Essex, 1987, p. 302.
- [12] R. H. Weber, Ph. D. Thesis, University of Basel, 1988.
- [13] A. J. Rippert, H.-J. Hansen, *Helv. Chim. Acta* **1993**, *76*, 2906; R. Hunziker, D. Sperandio, H.-J. Hansen, *ibid.* **1995**, *78*, 772.
- [14] a) A. A. S. Briquet, H.-J. Hansen, *Helv. Chim. Acta* **1994**, *77*, 1940; b) A. A. S. Briquet, P. Uebelhart, H.-J. Hansen, *ibid.* **1995**, in preparation.
- [15] Y. Chen, R. W. Kunz, P. Uebelhart, R. H. Weber, H.-J. Hansen, *Helv. Chim. Acta* **1992**, *75*, 2447.
- [16] G. L. Knaup, Ph. D. Thesis, Technische Hochschule Darmstadt, 1985.
- [17] K. Abou-Hadeed, H.-J. Hansen, unpublished results.
- [18] S. H. Pine, *Org. React.* **1993**, *43*, 1.
- [19] H. Günther, 'NMR Spektroskopie', 3rd edn., Georg Thieme Verlag, Stuttgart, 1992, p. 103 ff.
- [20] J. M. Read, C. T. Mathis, J. H. Goldstein, *Spectrochim. Acta* **1965**, *21*, 85.
- [21] Q. N. Porter, J. Baldas, 'Mass Spectrometry of Heterocyclic Compounds', Wiley-Interscience, New York, 1971, p. 107 ff.
- [22] P. Kouroupis, H.-J. Hansen, *Helv. Chim. Acta* **1995**, *78*, 1247.
- [23] W. Bernhard, H.-R. Zumbrennen, H.-J. Hansen, *Chimia* **1979**, *33*, 324.